Reobservations on ordering, precipitation and polymorphic phase transformation phenomena during annealing of a severely cold rolled magnetic Fe-Co-10V alloy

Mohammad R. Kamali , Ali R. Mashregi , L. Pentti Karjalainen , Saeed Hasani , Vahid Javaheri , Sami Saukko , Jukka Kömi

PII: S2589-1529(20)30182-4
DOI: https://doi.org/10.1016/j.mtla.2020.100765
Reference: MTLA 100765

To appear in: *Materialia*

Received date: 7 March 2020
Accepted date: 1 June 2020

Please cite this article as: Mohammad R. Kamali , Ali R. Mashregi , L. Pentti Karjalainen , Saeed Hasani , Vahid Javaheri , Sami Saukko , Jukka Kömi , Reobservations on ordering, precipitation and polymorphic phase transformation phenomena during annealing of a severely cold rolled magnetic Fe-Co-10V alloy, *Materialia* (2020), doi: https://doi.org/10.1016/j.mtla.2020.100765

Highlights:

- The order-disorder transition is reported also for austenite
- Precipitation starts concurrent with austenite formation, then particles dissolve
- Two temperature intervals determined for austenite transformation
- Contributions of vanadium partitioning and grain size to austenite stability were estimated

Reobservations on ordering, precipitation and polymorphic phase transformation phenomena during annealing of a severely cold rolled magnetic Fe-Co-10V alloy

Mohammad R. Kamali[a,1], Ali R. Mashregi[b], L. Pentti Karjalainen[c*], Saeed Hasani[d], Vahid Javaheri[e], Sami Saukko[f], Jukka Kömi[g]

Mohammad Reza Kamali[a]

[a]Materials and Mechanical Engineering unit, Centre for Advanced Steels Research, Box 4200, University of Oulu, FI-90014 Oulu, Finland.

[1]Department of Mining and Metallurgical Engineering, Yazd University, Yazd, Iran. Mr.kamaliardakani@yahoo.com; mohammad.kamali@oulu.fi

Ali Reza Mashreghi[b]

[b]Department of Mining and Metallurgical Engineering, Yazd University, Yazd, Iran. amashreghi@yazd.ac.ir

Leo Pentti Karjalainen[c]

[c]Materials and Mechanical Engineering unit, Centre for Advanced Steels Research, Box 4200, University of Oulu, FI-90014 Oulu, Finland. pentti.karjalainen@oulu.fi

Saeed Hasani[d]

[d]Department of Mining and Metallurgical Engineering, Yazd University, Yazd, Iran. hasani@yazd.ac.ir

Vahid Javaheri[e]

[e]Materials and Mechanical Engineering unit, Centre for Advanced Steels Research, Box 4200, University of Oulu, FI-90014 Oulu, Finland. vahid.javaheri@oulu.fi

Sami Saukko[f]

[f]Centre for Material Analysis, University of Oulu, FI-90014 Oulu, Finland. sami.saukko@oulu.fi

Jukka Kömi[g]

[g]Materials and Mechanical Engineering unit, Centre for Advanced Steels Research, Box 4200, University of Oulu, FI-90014 Oulu, Finland. jukka.komi@oulu.fi

Corresponding Author:

* L. Pentti Karjalainen, Materials and Mechanical Engineering unit, Centre for Advanced Steels Research, Box 4200, University of Oulu, FI-90014 Oulu,

Finland.

E-mail address: pentti.karjalainen@oulu.fi

Tel: +358 40 7047475

Reobservations on ordering, precipitation and polymorphic phase transformation phenomena during annealing of a severely cold rolled magnetic Fe-Co-10V alloy

Mohammad R. Kamali[a,b], Ali R. Mashregi[b], L. Pentti Karjalainen[a,*], Saeed Hasani[b], Vahid Javaheri[a], Sami Saukko[c], Jukka Kömi[a]

[a]Centre for Advanced Steels Research, University of Oulu, FI-90014 Oulu, Finland

[b]Department of Mining and Metallurgical Engineering, Yazd University, Yazd, Iran

[c]Centre for Material Analysis, University of Oulu, Fi-90014 Oulu, Finland

Abstract

Despite extensive investigations conducted on magnetic Fe-Co-V alloys, some aspects of microstructural evolution during annealing of cold rolled sheets have not yet been clarified yet. Various techniques such as dilatometry, X-ray diffraction (XRD), transmission and scanning electron microscopy (TEM, SEM) as well as ThermoCalc predictions were employed to study ordering, precipitation and austenite transformation in an 86% cold-rolled 40Fe-50Co-10V alloy. Dilatometric results revealed atomic ordering initiated from disordered martensite at 350 °C, while XRD patterns ascertained the completion of the process at 600 °C and its disappearance close to 750 °C. X-ray and electron diffraction patterns exhibited the B2 type ordered structure in this temperature range. Rod-shaped precipitates with HCP crystalline structure and the constant composition of $(Co,Fe)_3V$ were detected by SEM within the deformed ferrite grains after annealing in the temperature range of 500–700 °C. The percentage of the precipitates decreased by raising the annealing temperature and they vanished above 700 °C, in accordance with ThermoCalc prediction. Austenite grains formed below 750 °C had an ordered $L1_2$-type structure as revealed by TEM and XRD patterns. A combination of different techniques demonstrated that the two-phase ferrite-austenite region exists in the temperature range of 495–840 °C. Vanadium partitioning into

austenite during isothermal holding in addition to austenite grain size were evaluated as the main parameters affecting austenite stability during quenching from temperatures between 500–800 °C. As a final result, most of the existing disagreements and ambiguities in previous works could be explained.

Keywords: Fe-Co-10V alloy, microstructural characterization, ordering, precipitation, austenite transformation, austenite stability, partitioning

1 Introduction

The phase and microstructural evolution in equiatomic Fe-Co alloys containing small amounts of vanadium have been extensively studied because of their importance as soft magnetic materials [1–4]. However, the vanadium content in the range of 6–16% (all compositions are in wt.%, if not mentioned otherwise) increases the coercive force so that Fe-Co-V alloys can be classified as semi hard and hard magnetic materials due to the microstructural changes imposed by vanadium alloying as well as annealing conditions. For example, the coercive force of a 90% cold rolled Fe-Co-7.15V alloy has found to vary between 3.0 and 11.0 kA/m after various heat treatments [5]. Therefore, to determine the optimal heat treatment conditions for a certain alloy, investigating microstructural evolution during heat treatment and knowing the relationship between the microstructure and properties is crucial.

There are two main transformation processes in the Fe-Co binary system, allotropic (austenite (γ) $\rightleftharpoons$ ferrite (α)) and atomic ordering reactions, from which the later destroys the mechanical properties of the alloy [6]. Therefore, alloying elements, mostly vanadium, are always employed to enhance room temperature ductility [7]. Vanadium

not only affects mechanical properties, but also changes magnetic properties of the binary alloy significantly. Such changes in magnetic properties are due to the influence of vanadium in lowering the temperature of allotropic transformation as well as formation of Co_3V precipitates [1,8]. However, this element does not change the critical temperature of the ordering transformation (T_C) significantly, for this temperature is determined mostly by the Fe to Co ratio [9]. For the same values of Fe and Co content in the alloys, T_C lies around 730 °C and ordering transformation takes place in the range of 29–70 at.% of Co [1].

Despite extensive research associated with phase analysis and microstructural examinations on Fe-Co-V alloys so far, there are still inconsistent reports in the literature. This can be attributed to the simultaneous occurrence of some completely different phenomena including atomic ordering, precipitation (formation of $(Co,Fe)_3V$ particles), allotropic transformation, and recrystallization in the cold-rolled Fe-Co-V based alloys which makes it difficult to examine each phenomenon separately.

Recrystallization of a cold rolled Fe-Co-10V alloy was investigated recently by the present authors and it was revealed that this phenomenon takes place by a continuous mechanism with significant difference in the recrystallization rate under the ordered and disordered states [10]. However, the recrystallization kinetics was found to follow the Avrami-type kinetics with a constant exponent in both the ordered and disordered regions.

The ordering transition for BCC matrix in binary (Fe-Co) and ternary (Fe-Co-V) systems has been extensively investigated and results reviewed by Sundar and Deevi [1]

and Sourmail [2]. However, the ordering reaction in the austenite (FCC phase) has not received much attention yet and the ordered austenite has been mostly considered as ordered precipitates at low temperatures [11–15].

As can be seen in the phase diagram reported by Sourmail [2] based on several studies, vanadium alloying expands the two-phase intercritcal region and decreases the transformation temperature. In spite of extensive research dedicated to determine the phase temperature intervals of polymorphic transformation in Fe-Co-V alloys [4,9,11,16–18], still significant inconsistences exist concerning the values [2,9,18]. For instance, for an Fe-Co-7V alloy, the allotropic transformation was not verified below 750 °C using dilatometric tests and magnetization measurements by Zakharov et al. [18], whereas Hasani et al. [9] reported a wide temperature range of 480–920 °C as the two-phase region for an alloy with the similar composition [9].

In addition to the allotropic transformation, precipitation seems to be another unclear phenomenon during heat treatment of Fe-Co-V based alloys and can be mixed with the austenite phase transformation. Chen [19] could not find evidence for the existence of the austenite phase in an Fe-49Co-2V alloy below 700 °C using dilatometry, metallography and XRD techniques. Contrarily, Fiedler and Davis [12] reported austenite precipitates in a similar alloy after annealing at 680 °C. Bennett and Pinnel [4] argued that in an equiatomic Fe-Co alloy containing 2.5–3%V, austenite can precipitate at 600 °C through decomposition of a non-equilibrium BCC ferrite phase (martensite) into an ordered bcc phase and stabilized austenite. Existence of blocky Co_3V precipitates has been reported by Hasani et al. [20] in an Fe-Co-7.15V alloy while no precipitation phenomenon was observed in the study of Zakharov et al. [18] for a

similar alloy. Zel'dovich et al. [15,21] have reported two kinds of morphology for precipitates in an Fe- 52.9Co- 10.6V, namely rod-shaped and broad plates (equiaxed), formed inside and on boundaries of martensite laths respectively. For an Fe-Co-2V alloy, Ashby et al. [3] proposed that an iron-substituted Co_3V compound, $(Co,Fe)_3V$ with $L1_2$ (ordered FCC) structure, grows as rods along the ⟨111⟩ direction of ferrite matrix in the temperature range of 477–627 °C. Further, Sundar and Deevi [22] observed $(Co,Fe)_3V$ precipitates during annealing of an Fe-Co-4.5V alloy below 750 °C.

It is obvious, thus, that although many studies have been devoted to investigating the Fe-Co-V based alloys, some aspects of microstructural evolution during annealing of these alloys have remained unclear so far. Therefore, extended analysis including a dilatometric run, X-ray diffraction (XRD), electron backscatter diffraction (EBSD) and scanning (SEM) and transmission electron microscopy (TEM) examinations together with ThermoCalc software predictions were employed to study the phenomena occurring during annealing a severely cold rolled 40Fe-50Co-10V alloy.

2 Material and experimental procedures

2.1 Material and processing

The material used in this study was an Fe-Co-V based alloy with the exact chemical composition determined by the inductively coupled plasma mass spectrometry which is presented in Table 1. To ensure low impurity levels, pure raw materials charged in a vacuum arc furnace including a non-consumable electrode. For melting, the furnace was purged three times with pure Ar gas and evacuated afterwards. Electric arcing, finally, initiated under 500 mb pure argon gas. To guarantee the melt homogeneity, the melting

step was repeated five times and then cast into a closed bottom water-cooled copper mold with internal dimensions of 10×30×100 mm.

Table 1. Chemical composition of the studied alloy.

Element	Co	Fe	V	Cr	Mn	Zn	C	P	S
Amount (wt.%)	49.8	40.1	9.96	0.06	0.009	0.002	0.002	0.01	0.001

In order to modify the as-cast structure, the three ingots obtained were subjected to a homogenizing process at 1200°C for 10 hours and subsequently quenched in water to prevent ordering transformation. For obtaining desirable final thickness, the alloy was first hot rolled to a thickness of 1 mm (90% thickness reduction) under a temperature range of 950–850 °C in the austenitic region (according to dilatometric curve, given later in Fig. 1), followed by cold rolling to a thickness of 0.14 mm (86% thickness reduction). Afterward, specimens were annealed in a vacuum atmosphere, heated at a rate of 5 °C/s up to 450, 500, 550, 600, 650, 700, 750, 800 and 850°C for various durations between 10 and 240 min, and then cooled at a rate of 10 °C/s via high purity argon gas flow. Annealed samples were coded regarding annealing temperature (°C) – time (min) condition, for instance, 550-120 min represents a sample annealed at 550 °C for 2 hours.

2.2 Material characterization

Dilatometric tests were carried out using a DIL 805 A/D dilatometer (BAHR, Germany) to study the dimensional changes related to the phenomena occur during heating and cooling of the material under study. The dilatometric sample was prepared in the form of cylinder with a diameter of 4 mm and a height of 10 mm. The sample was heated to a peak temperature of 1000 °C under vacuum atmosphere at the rate of 10 °C/min, held

for 15 min and cooled to the ambient temperature at the same rate by means of a continuous flow of argon gas.

A Rigaku Smart Lab 9 kW X-ray diffractometer with a Co rotating anode operated at 40 kV and 135 mA in the back-reflection mode and a step size of 0.02° was utilized for accurate phase analysis. In order to remove the effect of texture on X-ray reflections, measurements were carried out using the average of seven different angles.

For microstructural examination, annealed samples measured 1*0.5*0.14 mm were etched in a 2.5% $FeCl_3$ solution after mechanical polishing down to 0.25 μm finish by a diamond paste. For specific purposes, deep etching was applied to dissolve ferrite. Microstructures were examined using a Zeiss Sigma field emission SEM equipped with an EBSD detector. EBSD runs were carried out using an accelerating voltage of 15 kV, a working distance of 15 mm, a tilt angle of 70° and a step size of 0.03 μm. SEM secondary electron imaging was used under an accelerating voltage of 5 kV and a working distance of 5 mm, because it yielded a better resolution than the EBSD did.

TEM imaging and electron diffraction were conducted using a 200 kV energy filtered scanning transmission electron microscope (JEOL JEM-2200FS EFTEM/STEM). Thin foils for TEM analyses were prepared using the focused ion beam (FIB) technique. Also, imaging and elemental mapping were conducted using bright field imaging mode in scanning TEM (STEM) mode with JEOL Dry SD100GV EDS detector. Quantitative results from the collected EDS maps sized 256 × 256 pixels were calculated using a JEOL Analysis Station software. Chemical composition of different phases were estimated using semi-quantitative standardless thin-film approximation.

Thermodynamic calculations for the phase diagram were made using the commercial Thermo-Calc software package including TCFE9 database [23].

3 Results

3.1 Dilatometric test

In order to determine the temperature ranges where certain phenomena occurred, the length change ($\Delta L/L_0$) of the sample was recorded as a function of temperature during continuous heating at 10 °C/min from room temperature to 1000 ºC, holding for 15 minutes and followed by continuous cooling to room temperature at the same rate. A typical dilatometric curve is presented in Fig. 1. For better clarifications, the total curve has been divided into four sections shown by enlarged sections of the curves. The deviations from the straight trace, indicated by tangent lines, have been used for determining the critical temperatures. The first region (section I) with a slight increase in on-heating expansion starts at 350 ºC and continues till 495 ºC. Just above this temperature, the slope of the curve decreases and until 550 ºC, where changes become negative (section II). The next change in the slope is seen above 635 ºC so that once again it becomes positive above 650 ºC (section III). This trend continues with an incessant slope till 750 ºC where one can witness the next contraction. After a short negative trace above 760 ºC, the slope of the curve declines at 778 ºC followed by a slight positive trend up to 810 ºC. The last section (section IV), which shows a pronounced contraction in the temperature range of 810–840 °C, is followed by continuous thermal expansion up to 1000 °C. After 15 minutes holding at 1000 °C, during cooling the sample contracts continuously up to

280 °C, where a sharp expansion starts and finishes at around 100 °C. Further cooling to room temperature demonstrates nothing but continuous contraction.

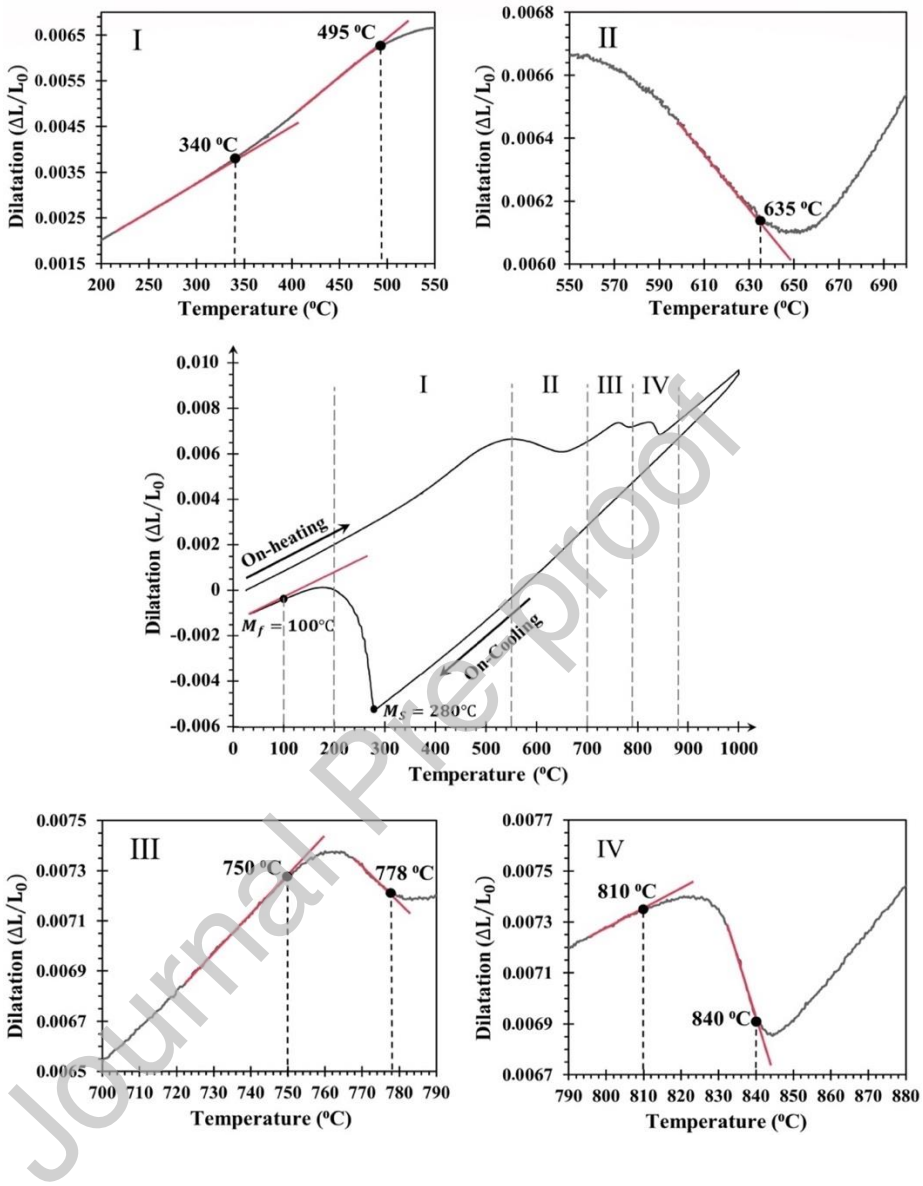

Fig. 1 Plot of dilatation as a function of temperature for the studied alloy at the heating and cooling rate of 10 °C/min.

3.2 XRD Analysis

The XRD patterns of the cold-rolled sample and specimens annealed at various temperatures for the duration of 120 min are displayed in Fig. 2. Chon et al. [24] have reported that ordering superlattice reflections are visible at 2θ = 36.5º and 65.7º

associated with (100) and (111) planes, respectively. The XRD patterns of annealed samples at temperatures higher than 500 ºC show indications of the superlattice reflections at those positions, better seen in Fig. 2b. Some slight bulges are visible at 500 ºC at the mentioned angles increasing up to the highest intensity at 600 ºC, following by a constant decline until 700 ºC and finally the reflections disappear at 750 ºC and above.

The FCC austenite peaks appear in sample annealed at 550 °C and their intensity increase with increasing the annealing temperature reaching a maximum at 750 ºC. At still higher temperatures, the intensity of austenite reflections decreases and finally disappears at 850 ºC, where only the reflections for the BCC ferrite phase remain. It should be noticed that the reflections associated with the superlattice formation of the austenite are seen in the temperature range of 600–700 ºC and $2\theta = 41.5^{o}$, where considerable amount of austenite is formed. With raising temperature, the superlattice reflection related to this phase weakens up to 700 ºC, and no relevant reflection is detected in the pattern of 750 ºC.

As a new phenomenon, reflections at $2\theta = 48.6^{o}$ and 56.5^{o} (Fig. 2b) were observed, which do not account for neither BCC nor FCC structures, but they can be dedicated to the HCP crystal structure , known as the structure of the pure Co_3V compound [25]. Therefore, XRD results suggest that the formation of a hexagonal phase with the composition of Co_3V could occur at temperatures 550 –650 ºC, where some Co atoms can be replaced by Fe atoms [1].

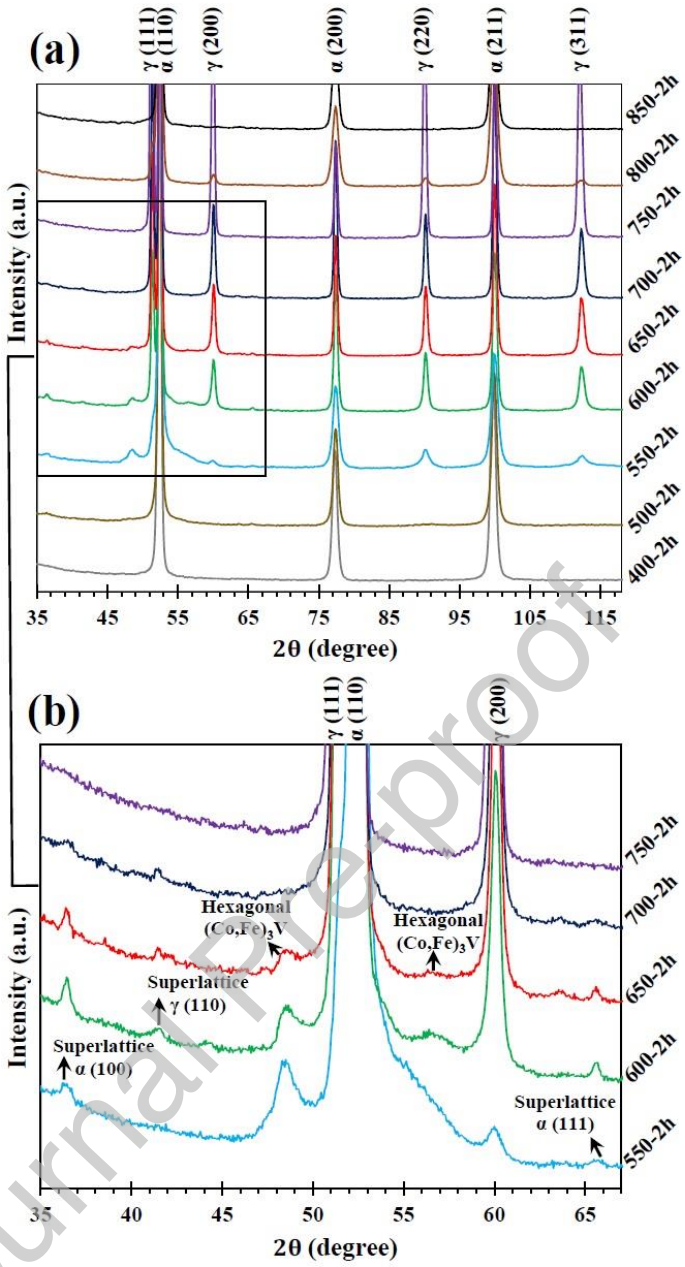

Fig. 2 (a) Room temperature XRD patterns of samples annealed at different temperatures for 120 min (b) higher magnification of a selected area from (a).

3.3 EBSD examinations

Microstructure of the cold rolled sample as well as the annealed and cooled ones were examined by SEM-EBSD to detect the existing phases. EBSD (phase + image quality (IQ)) maps related to the cold rolled and annealed samples at different temperatures for 120 min soaking time are illustrated in Fig. 3. Owing to the disability of EBSD to recognize very fine austenite grains especially at lower temperatures, the 120 min

duration was selected for enough austenite grain growth. Also, longer soaking times were considered to lower the austenite stability at room temperature.

Two kinds of ferrite grains can be distinguished in Figs. 3b and 3c (and 3e), lighter grains and darker ones. The difference in the image quality (IQ) is related to different dislocation density in those regions; a higher dislocation density suggests lower IQ and a darker area in an IQ map [26,27]. This variation reflects the recovery (Fig. 3b) and start of recrystallization (Fig. 3c) in deformed ferrite, as reported earlier by the present authors [10]. Due to recrystallization, the grain structure is obviously finer after annealing at 650 °C than annealing at 550 °C.

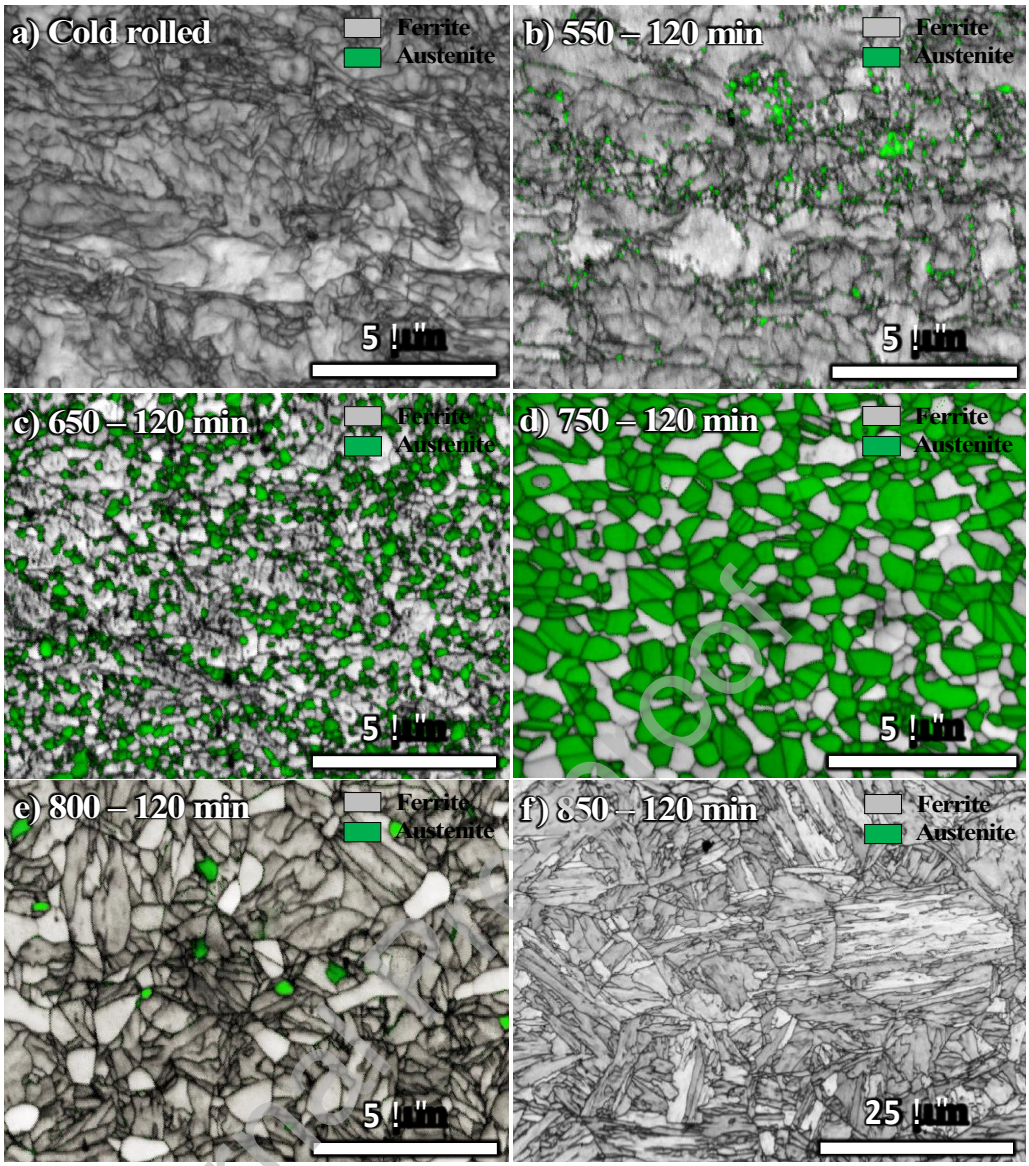

Fig. 3 Room temperature EBSD Phase + IQ maps of (a) a cold-rolled sample and samples annealed for 120 min at (b) 550 °C (c) 650 °C, (d) 750 °C, (e) 800 °C and (f) 850 °C.

The EBSD phase map demonstrates single phase ferrite/martensite in as cold rolled condition (Fig. 3a) and formation of austenite with few fine grains at 550 °C (Fig. 3b), whereas no austenite grains were detected after annealing at 500 °C and below (the figures not shown here). This observation is qualitatively consistent with dilatometric and XRD results revealing the existence of austenite at 550 °C. The fractions of retained austenite at room temperature under various annealing conditions are presented in Table 2. The fraction of the austenite phase increased with increasing the annealing

temperature reaching a maximum at 750 ºC, then decreasing so that no austenite phase was observed at room temperature after annealing at 850 ºC. The fraction also increased with increasing the annealing time at temperatures up to 700 °C, reached a maximum after 60 min annealing at 750 °C but decreased at 800 °C.

After annealing at 750 °C, the fraction of austenite is higher than that of ferrite and grains are equiaxed with high IQ (Fig. 3c). In the sample annealed at 800 ºC (Fig. 3d), few austenite grains are present, and the BCC phase distinctly consists of two kinds of grains with different degrees of IQ. The grains with high IQ are similar in shape as in Fig. 3c (recrystallized ferrite grains with low dislocation density), but the grains with low IQ are lenticular in shape or consists of several laths. These grains are martensite, as can also be concluded from the dilatometric curve (Fig. 1). It is well known that martensite contains a high density of dislocations due to its diffusionless shear transformation. Thus, a portion of austenite formed at a high annealing temperature has transformed to martensite during cooling. In Fig. 3e, the entire structure is martensitic exhibiting lath morphology and a coarse prior austenite grain size.

The stability of austenite against martensitic transformation during cooling from high temperatures depends on several factors such as chemical composition and grain size [28–31], which are, in turn, dependent on annealing temperature and duration. Therefore, in order to analyze their contributions, the composition and austenite grain size were determined using the analytical TEM (section 3.4) and EBSD techniques respectively. The average grain size of the retained austenite after annealing for 120 min at various temperatures is presented in Fig. 4a. As seen, retained austenite grain size has grown with increasing the annealing temperature, and particularly annealing at 750 ºC

results in significant coarsening of the grain size. However, with heating at 800 ºC, retained austenite grains are finer, and no austenite is retained after annealing at higher temperatures. Although, it should be noticed that the austenite grain size seen after annealing at 800 °C does not present the grain size existed at the annealing temperature, but those grains are only pieces of larger grains, remained untransformed to martensite. Obviously, it means that the M_S and M_f temperatures (the start and finish temperature of martensite transformation during cooling from austenitic region, respectively) of the austenite after annealing at 800 °C are above and below room temperature respectively, but after annealing at 850 °C (fully martensitic structure), both are above. The dilatometric curve (Fig. 1) suggested M_f =100 °C for the austenite annealed at 1000 °C for 15 min.

The austenite grain size existed during annealing at various temperatures is plotted in Fig. 4b. For temperatures up to 750 °C, it is equal to that of the retained austenite, but at 800 °C (also at 750 °C for 240 min annealing), it is much coarser and not distinguishable directly from the EBSD image in Fig. 3d or 4a. The prior austenite grain size was obtained by measuring the grain size of transformed austenite in such a way that etching the microstructure leaded to disappearance of the initial ferrite grains owing to their low vanadium level, whereas martensite was resistant due to its high vanadium amount (see later Table 3). A typical SEM image of the polished and etched sample annealed at 800 °C for 120 min, is shown in Fig. 5. Also, the etchant solution was capable to reveal the prior austenite grain boundaries, and the absence of initial ferrite grains, made it possible to measure the average grain size of the prior austenite. The other method for determing the prior austenite grain size is measuring darker areas in an EBSD-IQ map which demonstrate transformed austenite to martensite regions. In this study both the procedures were employed, and the results were entirely consistent and

are illustrated in Fig. 4b. The same process was used to measure the volume fraction of the prior austenite, whereas the volume fraction of retained austenite was directly extracted from EBSD-phase maps. The results of measurements are presented in Table 2. As a comparison, ThermoCalc predictions concerning precipitates and austenite fractions are also represented in this table. Just to highlight, the trend of changes is shown in Fig 6. From Fig. 6a, it can clearly be seen that martensite is formed at 750 °C after 240 min annealing, whereas at 800 °C only 10 min would be enough for it to form. According to Fig. 6b, it could be observed that for annealing times longer than 60 min at 750 °C, the equilibrium condition is obtained and the volume fraction of prior austenite is remained constant. The amount of retained austenite for 60 min and 120 min annealing times is almost the same. Thus, instability of retained austenite and transformation to martensite is occurred for annealing times longer than 120 min. Comparing the volume fraction of prior austenite below and above 750 °C for all durations in Fig. 6b, the role of atomic order on the kinetics of austenite formation becomes evident. Further, Fig. 6b suggests that equilibrium conditions for austenite formation are achieved within 60 and less than 10 min in annealing at 750 and 800 °C respectively.

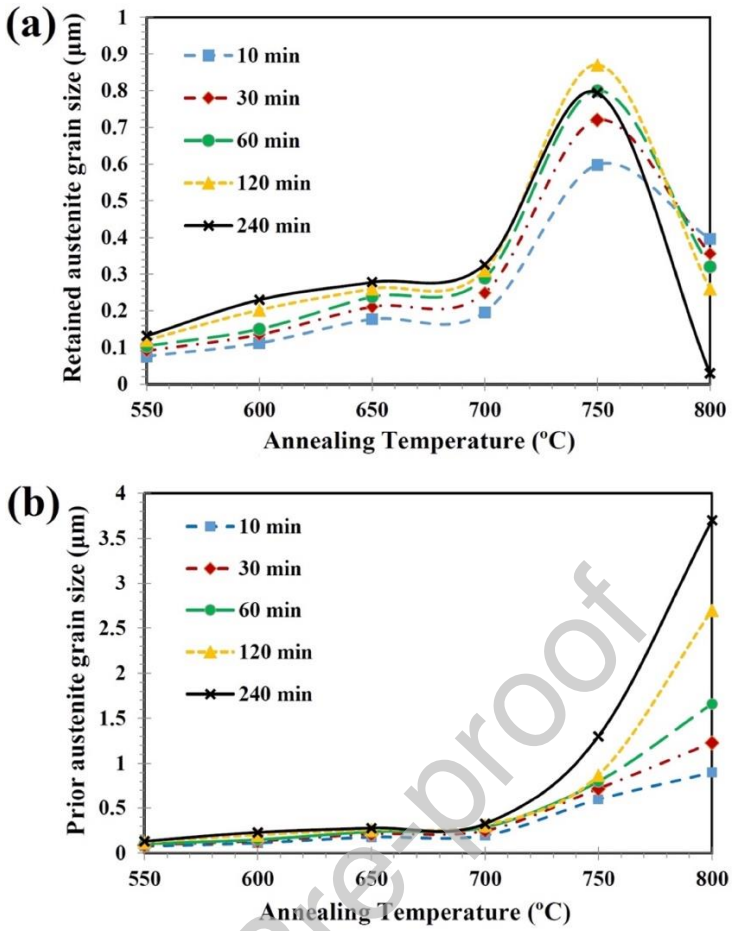

Fig. 4 Average grain size of retained (a) and prior (b) austenite after annealing under various conditions determined by EBSD.

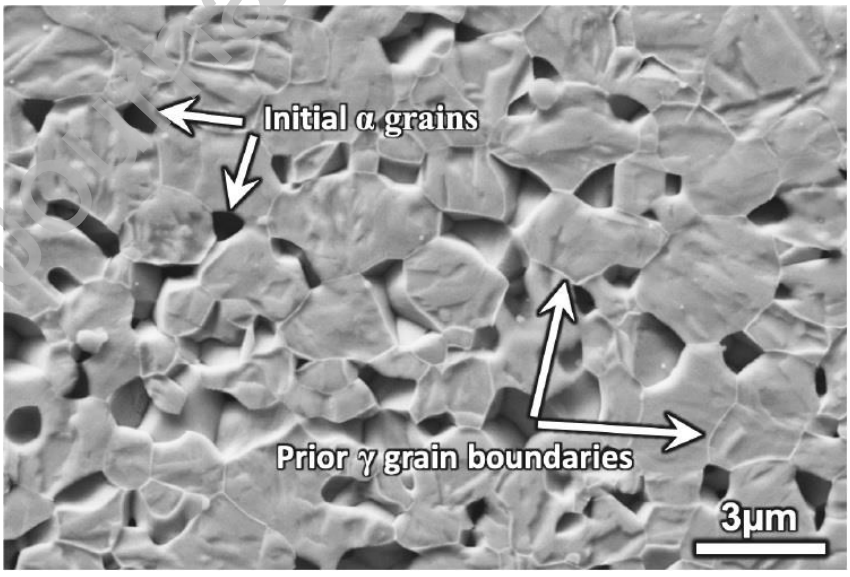

Fig. 5 SEM image of an etched 800-120 min sample showing deeply etched initial ferrite and prior austenite grains.

Table 2. Volume fraction of retained and prior austenite (in vol.%) after annealing under various conditions based on EBSD. ThermoCalc predictions incorporating $(Co,Fe)_3V$ precipitates (shown by *) are presented for comparison.

Annealing time (min)	Annealing temperature (°C)							
	550	600	650	700	750		800	
					Retained	Prior	Retained	Prior
10	0.6	3.8	12.8	17.7	58.5	58.5	10.8	~85
30	1.4	9.8	21.4	24.3	61.1	61.1	3.6	~85
60	1.9	12.5	22.3	26.7	63.8	~64	2.7	~85
120	4.1	16.6	24.5	28.1	63.6	~64	2.4	~85
240	6.5	19.9	28.9	31.8	46.1	~64	0.3	~85
ThermoCalc	13.8*	11.7*	9.4*	25.0		42.0		69.0

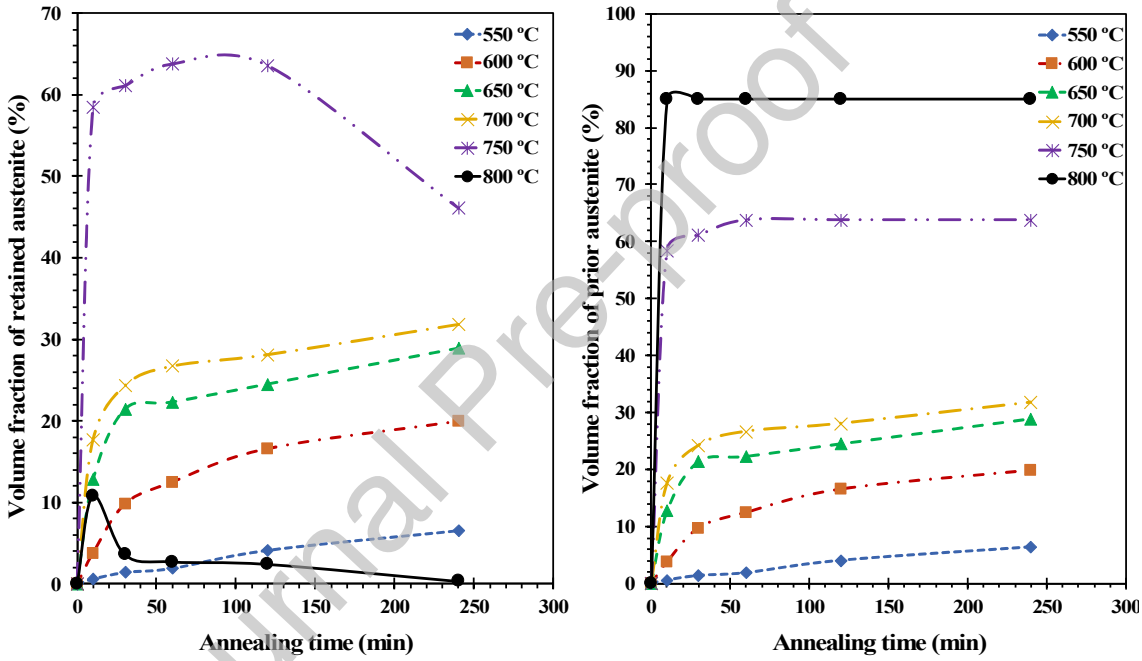

Fig. 6 Volume fraction of retained (a) and prior (b) austenite at high temperatures under various annealing conditions calculated from EBSD data assuming zero as the initial fraction of austenite.

3.4 TEM investigations

In order to determine the chemical compositions and crystal structures of the existing phases, TEM X-ray maps, showing the distribution of vanadium (V), iron (Fe) and cobalt (Co) elements, and the diffraction patterns of different phases were recorded. Fig. 7 displays the elemental maps on the samples annealed at different temperatures for 60 min after cold rolling, and the selected area electron diffraction (SAED) patterns of the

existed phases are displayed in Fig. 8. In this figure, α´, α, γ´, γ and γ_2 represent the ordered ferrite (B_2 lattice structure), disordered ferrite/martensite (BCC), ordered austenite ($L1_2$), disordered austenite (FCC) and precipitates (HCP) respectively. Comparing the elemental maps and diffraction patterns, it could be concluded that during annealing V and Co diffuse simultaneously from ferrite/martensite to austenite, while Fe diffuses in the reverse direction. Table 3 presents the contents of these elements in ferrite, austenite and precipitates at various temperatures based on at least 5 measurements in each sample. As observed from Fig. 7 (a-d), in addition to ferrite, grains with two kinds of morphology, equiaxed and fibrous (rod-like), enriched of V and Co, coexisted at 600 and 650 ºC, while only equiaxed grains had remained in samples annealed at higher temperatures.

SAED patterns in Fig. 8(a-d) reveal superlattice diffraction spots for the austenite phase after annealing at 600, 650 and 700 ºC, but there are no such spots in the electron diffraction pattern of the specimen annealed at 750 ºC. Some spots which observe in the pattern of 750-60 min sample, are not superlattice diffractions, because they do not lie exactly on the straight line with main diffraction spots (red line in Fig. 8(d)). This indicates that the austenite phase has the ordered FCC ($L1_2$) structure while annealing below 750 ºC, but at 750 ºC and above, the austenite has the simple FCC lattice structure. Besides, it is clearly seen in Figs. 8c and 8d that, similarly as for the austenite, the superlattice diffraction spots of the ferrite disappeared in annealing at temperatures 750 ºC and above.

Furthermore, a considerable number of small precipitates (γ_2) which are found to be formed during annealing, represent the stoichiometric chemical composition of

$(Co,Fe)_3V$ (Table 3) and the HCP crystal structure. High density of mentioned precipitates is illustrated in Fig. 9, where higher magnification image is presented for more clarification. The composition was determined using an analytical TEM. The exact crystal structure of fine film-like (rod-shaped) precipitates is difficult to determine, because they are always embedded in the ordered BCC phase and the diffraction patterns of precipitates and ferrite overlap. For example, Fig. 8b depicts the spots related to the {110} planes of BCC matrix surrounded by other diffraction spots of the hexagonal precipitate. However, it was found that the BCC phase disappeared during a deep etching so that only precipitates and austenite remained. Therefore, the etched region in TEM analysis enabled us to unambiguously determine the crystal structure of very fine particles. Figs. 8a and 8a´ show the unetched and etched areas of the sample annealed at 600 ºC for 60 min respectively. It should be reminded that the Co, Fe and V content of the present alloy is 50, 40 and 10 wt.% respectively equivalent to 48.65, 41.09 and 10.26 at.%. Here, it is seen that after annealing at 600 ºC, pronounced partitioning of the elements has occurred, so that the ferrite is enriched with Fe and depleted of V, whereas the opposite has occurred in the austenite. With increasing the annealing temperature, Co and V contents of the austenite decreased but Fe increased. However, the changes in elemental contents in the ferrite are not considerable. In addition, the γ_2 precipitates have the identical stoichiometric composition both at 600 and 650 ºC, even though according to Figs. 7(a,b) and 8(a,b), the size of these precipitates increases with increasing the annealing temperature.

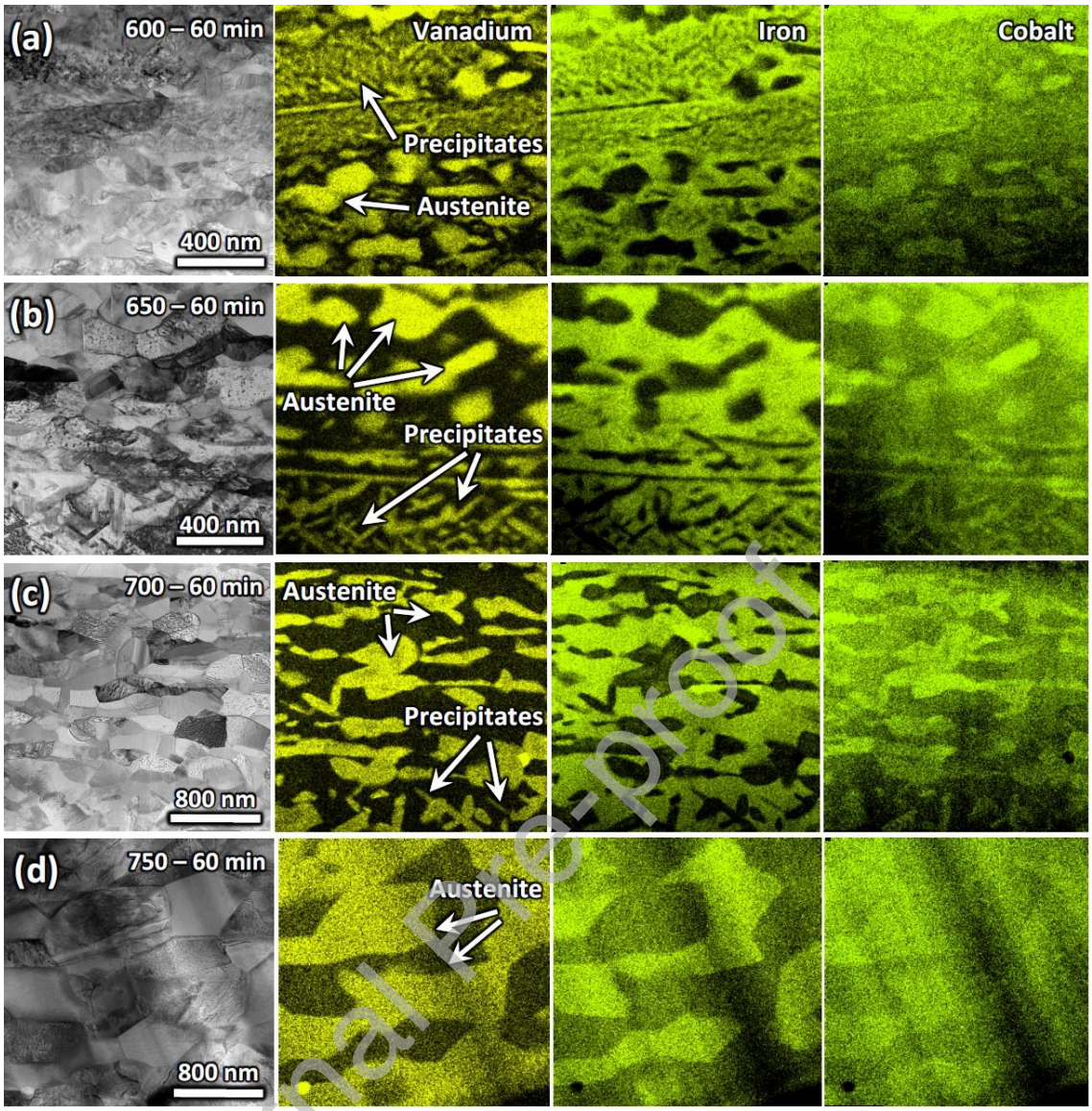

Fig. 7 TEM elemental maps of samples annealed for 60 min at (a) 600 °C, (b) 650 °C, (c) 700 °C and (d) 750 °C.

Table 3. Chemical composition of the existed phases at different annealing temperatures.

Sample	Phase compositions (at. %)								
	α'/α			γ'/γ			γ_2		
	Fe	Co	V	Fe	Co	V	Fe	Co	V
600-60 min	52-53	43-44	4-5	18-19	57-58	24-25	14-15	60-61	25-26
650-60 min	53-54	43-44	2-4	21-22	56-57	21-22	15-16	60-61	24-25
700-60 min	50-53	43-45	3-5	25-26	55-56	19-20	—	—	—
750-60 min	50-51	44-45	4-5	34-35	51-52	13-14	—	—	—

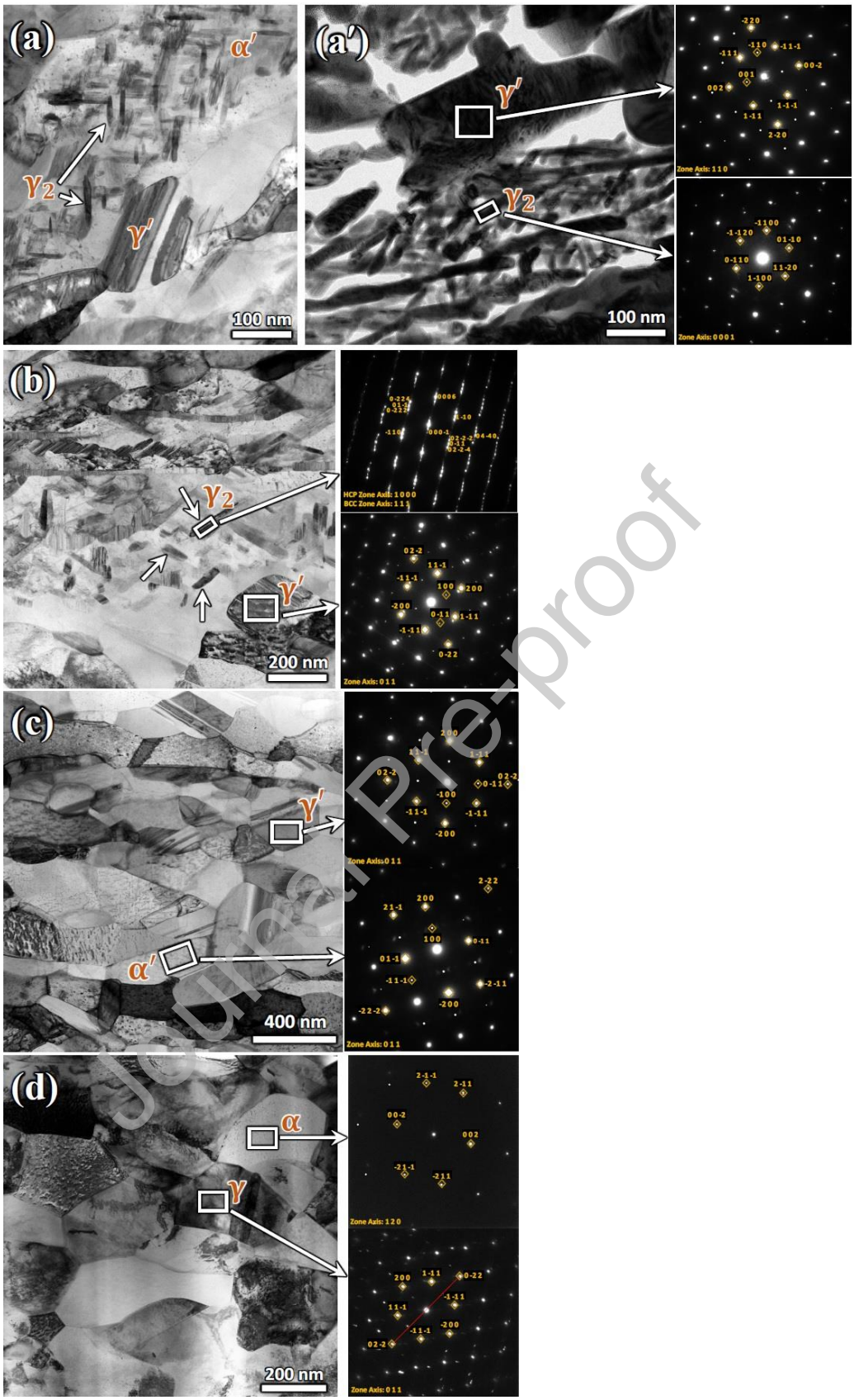

Fig. 8 TEM images together with SAED patterns of samples annealed for 60 min at (a,a´) 600 °C, (b) 650 °C, (c) 700 °C and (d) 750 °C. (a) presents the unetched region whereas (a') the etched region.

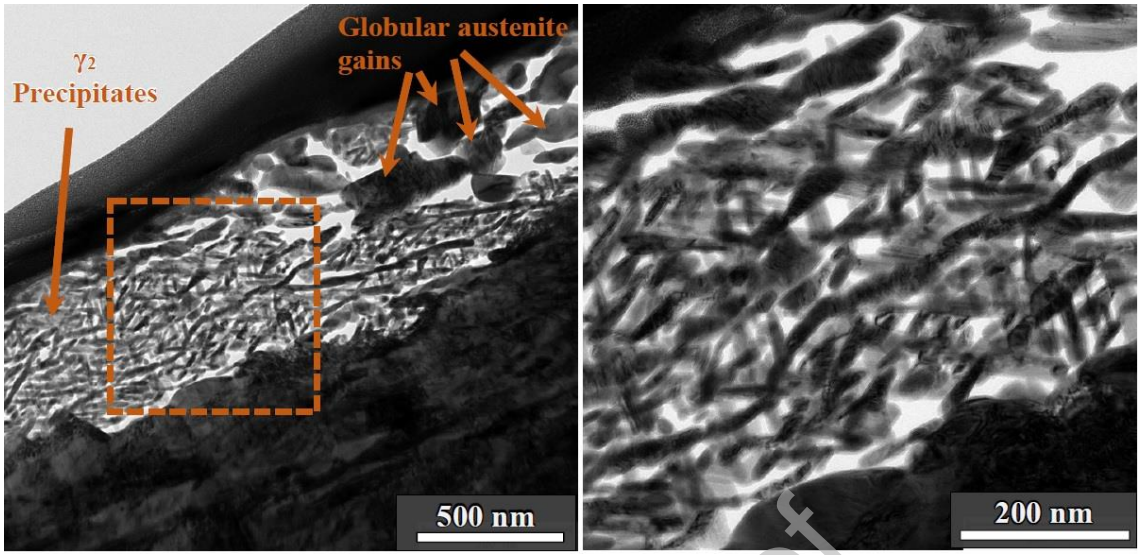

Fig. 9 Typical TEM image of a sample annealed at 600 ºC for 60 min along with a higher magnification area of numerous rod-shaped γ_2 precipitates inside an elongated ferrite grain. Globular austenite grains formed at grain boundaries of ferrite are also shown.

3.5 SEM observations

XRD revealed the existence of $(Co,Fe)_3V$ precipitates in samples heat treated at 550–650 °C for 120 min, but not at 700 ºC, probably due to their low volume fraction. In addition, TEM samples prepared by FIB technique were very small and the volumes examined therefore very local which might not consist any precipitates at 700 ºC. The tiny precipitates could not be detected at any temperatures by the EBSD method due to insufficient resolution of this technique. However, a wider region that could be examined by the SEM secondary electron technique, enabled us to determine the distribution and size of the precipitates in some locations. Views of the samples annealed at 550, 600, 650 and 700 ºC are shown in Fig. 10 at two magnifications. The formation of huge number of nano-scale precipitates inside ferrite grains is visible in the instance of annealing at 550–700 ºC, whereas no precipitates were seen after annealing at 750 ºC (not shown). As already pointed out, ferrite grains have lower resistance to the etchant solution than the austenite phase and precipitates have. Clearly, the morphology

of the precipitates is rod-shaped with the thickness of around 5–15 nm and varying length, as in the sample annealed at 550 ºC for 120 min (Fig. 10a). The thickness of these precipitates after annealing at 600, 650 and 700 ºC for the same duration of 120 min is about 10–30, 30–70 and 70–140 nm respectively. Also, comparing the images in Fig. 10, the highest amount of precipitates seems to form in the sample annealed at the lowest temperature of 550 ºC, and the volume fraction of these particles decreases at the higher annealing temperatures. This observation is in good agreement with the XRD results.

In addition to the precipitates, austenite grains, marked by white arrows in Fig. 10, are visible as equiaxed grains along wide zones at ferrite grain boundaries. Contrary to the amount of precipitates, volume fraction of the austenite increases with increasing the annealing temperature. Further, it seems that austenite grains grow from boundaries and consume rod-shaped precipitates or precipitates themselves coalescence together and convert to austenite during prolonged heating. Black arrows in Fig. 10 show the occurrence of this phenomenon.

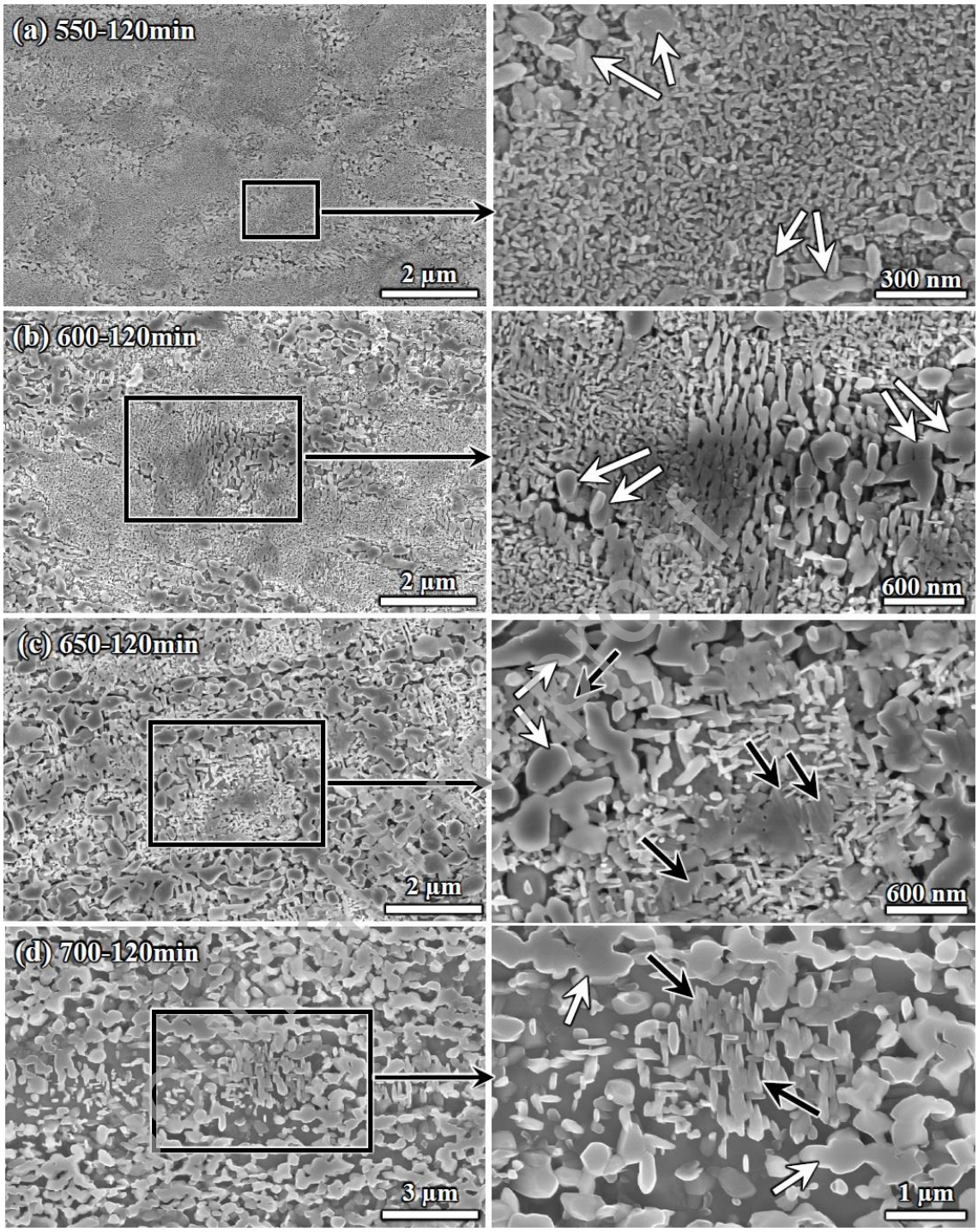

Fig. 10 SEM images of etched samples annealed for 120 min at (a) 550 ºC, (b) 600 ºC, (c) 650 ºC and 700 ºC together with selected areas shown at higher magnification. Rod-like precipitates and austenite grains are pointed by black and white arrows respectively.

For determining the start temperature of the precipitation or austenite formation, samples annealed at 500 ºC for different durations were examined using SEM. Fig. 11 displays microstructures of samples annealed at 500 ºC for 10 and 240 min as well as at

550 ºC for 10 min. Due to cold rolled conditions and just after the beginning of precipitation at 500 ºC, when the vanadium content of the ferrite/martensite has not decreased yet, the contrast, due to disappearance of ferrite grains, cannot be obtained and the resolution of the images is not desirable. However, recognizing the formation of precipitates as well as fine austenite grains is possible. As it is seen, traces of precipitates formed within 10 min at 500 ºC exist in the related image. Moreover, no austenite grains were observed under this annealing condition even focusing on different locations of the sample (figures not shown here). After 30 min, a few numbers of fine austenite grains were observed along grain boundaries while they proliferated and grew with increasing annealing time. However, further raising the annealing temperature to 550 ºC resulted in formation of numerous precipitates and austenite grains after 10 min (Fig. 11c).

We still observed a new phenomenon taking place. Fig. 12 displays the microstructure of a sample annealed at 850 ºC for 120 min, martensitic structure along with few micron-sized precipitate particles. EDS analysis revealed that these precipitates are V-rich compounds depleted of Fe and Co. According to the binary Co-V phase diagram, the only vanadium-rich precipitate stable below 1125 ºC, will be CoV_3 compound, [32,33]. Therefore, it could be concluded that these equiaxed vanadium-rich particles are CoV_3 precipitates formed during annealing at 850 or 950 °C (even at 800 °C but with lower amount). It should be mentioned that these particles were also observed in samples annealed at lower temperatures, but they were submicron in size and their number was very low, probably they formed during hot rolling before the cold rolling process.

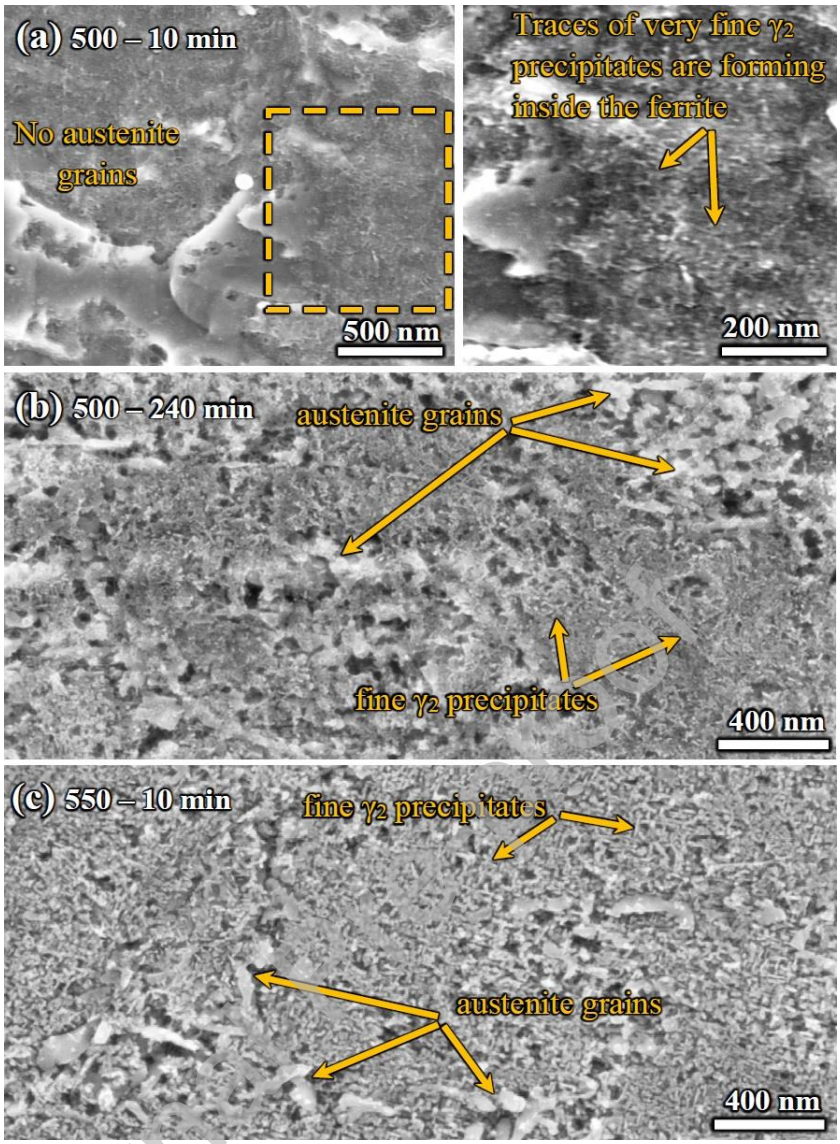

Fig. 11 SEM micrographs of (a) precipitates in the beginning stage of formation in sample annealed at 500 °C for 10 min, (b) precipitates and austenite grains which formed after 240 min annealing treatment at 500 °C, and (c) higher density of precipitates and austenite grains after annealing at 550 °C for 10 min.

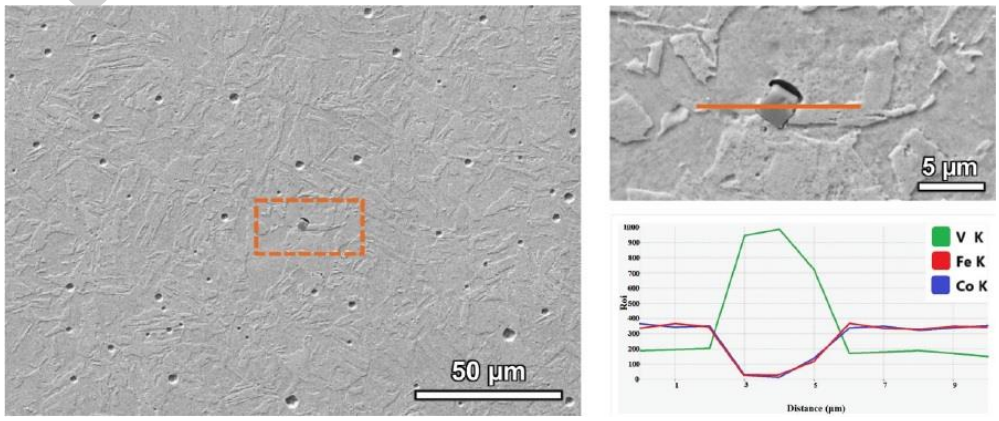

Fig. 12 SEM image of a martensitic sample after annealing at 850 °C for 120 min and cooling with EDS line scan of a precipitate.

4 Discussion

Simultaneously four phenomena including ordering, recrystallization, precipitation and polymorphic transformation take place during annealing a cold-rolled Fe-Co-10V alloy in a special temperature range which complicates examining each one separately. In the literature, there are inconsistent reports on Fe-Co-7V [9,18] as well as Fe-Co-(2-3)V alloys [3,4,12,34] which will be discussed in Section 4-4. For example, temperature intervals for the phase transformation vary considerably for similar compositions. Besides, the temperature range for precipitation, the lattice structure (FCC, $L1_2$ or HCP) and the morphology of the precipitates are unclear. This can be understood from the fact that it is quite difficult to distinguish the precipitates and fine austenite grains formed simultaneously during annealing at low temperatures.

Dilatometric experiments have been used earlier for various compositions in Fe-Co-V ternary system to determine different transformations [9,18,19]. However, it alone cannot reveal the phenomena that are taking place simultaneously. Combining various techniques makes it possible to resolve the problem and investigate each phenomenon in more detail. Recrystallization of ferrite was investigated in detail and stages clarified by the present authors recently [10]. Here, dilatometry, XRD, TEM, EBSD and SEM techniques were employed in order to examine other phenomena accurately and resolve the existing ambiguities. Also, ThermoCalc predictions were performed. The main observations and results will be discussed in the following sections.

4.1 Ordering transitions

It has been reported that the lattice parameter of ferrite slightly increases by the ordering transformation [1]. In a binary equiatomic Fe-Co alloy system, the growth

of the lattice parameter, caused by the ordering, has been shown to be 0.2% [35]. Accordingly, the first deviation in the slope of the dilatometric curve at 350 ºC (Fig. 1) can obviously be associated with the start of the ordering transition. Quite a similar result was obtained by Hasani et al. [9], who reported the temperature of 330 ºC as the starting temperature of the ordering transformation in a 90% cold rolled Fe-49.6Co-7.15V sheet under the same heating rate of 10 °C/min. Zakharov et al. [18] reported 400 °C as the ordering start temperature while heating a Fe-52Co-6.85V-0.3Mn-0.1Si alloy. These minor differences could be due to differences in the compositions of the tested alloys, sensitivity or the experimental scatter in dilatometric runs.

Concluding from the appearance of the ordering transition, the cold-rolled alloy, after water quenching from the homogenizing treatment (in the completely austenitic region) and before the heating or annealing treatment, has a fully BCC martensitic disordered structure. It should be noted that, looking at the alloy thermodynamically, its stable state at room temperature is the ordered structure [1]. During annealing ferrite/martensite, two types of order – disorder transitions can take place: i) gradually by nucleation and growth of the ordered domains or ii) the instant transition [36]. In the first case, material remains disordered through quenching from high temperatures and the restoration of the ordered state takes place during heating and develops gradually. However, in the second scenario, e.g. in Cu_3Au, the disordered state cannot be retained on quenching and there will be an abrupt change to high values of ordering at temperatures just below T_C [36,37].

According to Fig. 1, the slope of the dilatometric curve increases gradually with increasing the temperature up to 495 °C, reflecting the continuous accomplishment of the ordering transformation. In agreement with this dilatometric result, the intensity of the superlattice reflections increased gradually up to the annealing temperature of 600 ºC and then declined (Fig. 2b). Accordingly, it could be proposed that ordering transformation in the studied alloy takes place by the nucleation and growth mode, but it requires more detailed investigations to clarify. Hasani et al. [38] proposed that ordering transformation took place homogeneously at a moderate rate below 500 ºC and rapidly between 500–725 ºC in Fe-49.6Co-7.15V. But for an Fe-49.8Co-0·4%Cr alloy [39], Buckley argued that ordering transformation occurred in a homogenous manner between 475–725 ºC, but by nucleation and growth on grain boundaries below 475 ºC.

The superlattice XRD reflections of ferrite became visible on the samples annealed at 500 ºC. However, the initiation of ordering in the dilatometric recordings was seen already at 350 °C, suggesting that the ordering process starts as a short range order, which is known to occur at low temperatures (below 500 ºC) [40], yet hardly detectable by means of XRD. The ordering reflections are still present after annealing at 700°C but vanish for samples annealed at higher temperatures, which proves that the order – disorder transition takes place in the temperature range between 700 and 750 ºC (kinetics of ordering in Fe-Co and Fe-Co-V systems has been presented in a review by Sundar and Deevi [1]). Regarding this temperature range in the dilatometric curve (Fig. 1), it is seen that there is a gradual contraction starting at 750 ºC and finishing at 770 ºC (section III), which was attributed to the order–disorder transition in a previous study conducted by Hasani et al. [9].

However, according to XRD patterns (Fig. 2), the intensity of the order is not considerable at 750 ºC, and only the short range order has been found to exist around this temperature [40,41], which cannot be responsible for such a contraction. On the other hand, according to Table 2, it is seen that the fraction of austenite has significantly increased at 750 °C compared to that of 700 °C. It is known that mobility of boundaries follows a slow kinetics owing to formation of super-dislocations in ordered structures, even at temperatures where only short range order subsists [41–43]. Therefore, austenite transformation is slower in the ordered state than in the disordered state. Thus, the contraction at and above 750 ºC can not be attributed to the order–disorder transition but rather to fast austenite formation from the disordered ferrite. The temperature between 700 and 750 °C as the T_C temperature was determined according to the results from XRD and TEM. This temperature range is consistent with the Tc of 730 °C, reported for the binary 50Fe-50Co alloy [1], as well as 50Fe-48Co-2V (at.%) alloy according to Stoloff and Davies [41]. Thus, it can be concluded that the disordering temperature is not significantly dependent on the V content in Fe-Co-V alloys, a conclusion which has also been drawn by other researchers for various alloy compositions [1,9].

In addition to superlattice reflections of the ferrite phase, the corresponding reflections for the ordered austenite phase exist in the XRD patterns at around $2\theta=41.5°$ associated with the {110} planes. Consistently with this, also SAED patterns of austenite (Fig. 8) reveal superlattice diffraction spots for specimens annealed at the temperature range of 600–700 ºC. Thus, it can be concluded that the critical temperature of the ordering transition for the austenite (T_c^{γ}) lies between 700 and 750 ºC, similar to that of ferrite. To the best of authors knowledge this is the

first time that the order–disorder transition is reported for austenite and it has not earlier been suggested by other researchers. Moreover, it is reasonable to assume that the austenite phase forms at lower temperatures (around 500–600 ºC) as an ordered phase, but the amount of this phase is below the detection limit of XRD technique. It seems that there is a temperature range in which both the ferrite and austenite phases, and maybe HCP precipitates, are in the ordered state, though this requires more investigation for confirmation.

4.2 Allotropic transformation

It is well known that vanadium acts as an austenite stabilizer in Fe-Co alloys and vanadium addition decreases both the α/α+γ and α+γ/γ transition temperatures [2]. Depending on the vanadium content, the temperature intervals of the polymorphic and atomic ordering transformations can overlap, as already observed for the alloys containing 10.5% and 7.15% vanadium [9,18]. It also was reported that the ordering transition, recrystallization and austenite transformation overlap at temperatures above 500 °C, and single phase region of austenite phase lies above 840 ºC for an Fe-50C0-10V alloy [10].

Formation of two kinds of austenite, at low and high temperatures respectively, have been reported in some investigations, as reviewed by Sundar and Deevi [1] and Sourmail [2]. Hasani et al. [9] distinguished between low-temperature and high-temperature austenite based on some fluctuations in the dilatometric curve existing between the start and finish temperature of austenite transformation.

4.2.1 Two-phase region

In principle, phase transformation temperatures can be estimated from dilatometric recordings, XRD and microstructural observations, and they can be predicted using ThermoCalc software, for instance. However, pronounced scatter exists concerning the α/α+γ and α+γ/γ boundaries for Fe-Co-V alloys as discussed by Sourmail [2]. ThermoCalc software does not contain a proper database to predict their phase boundaries firmly. In Fig. 13a the equilibrium diagram of Fe-Co alloy based on ThermoCalc has been plotted as a function of V concentration. Fig. 13b presents approximately the same diagram with superimposed α/α+γ boundary on heating, taken from Sourmail's paper [2].

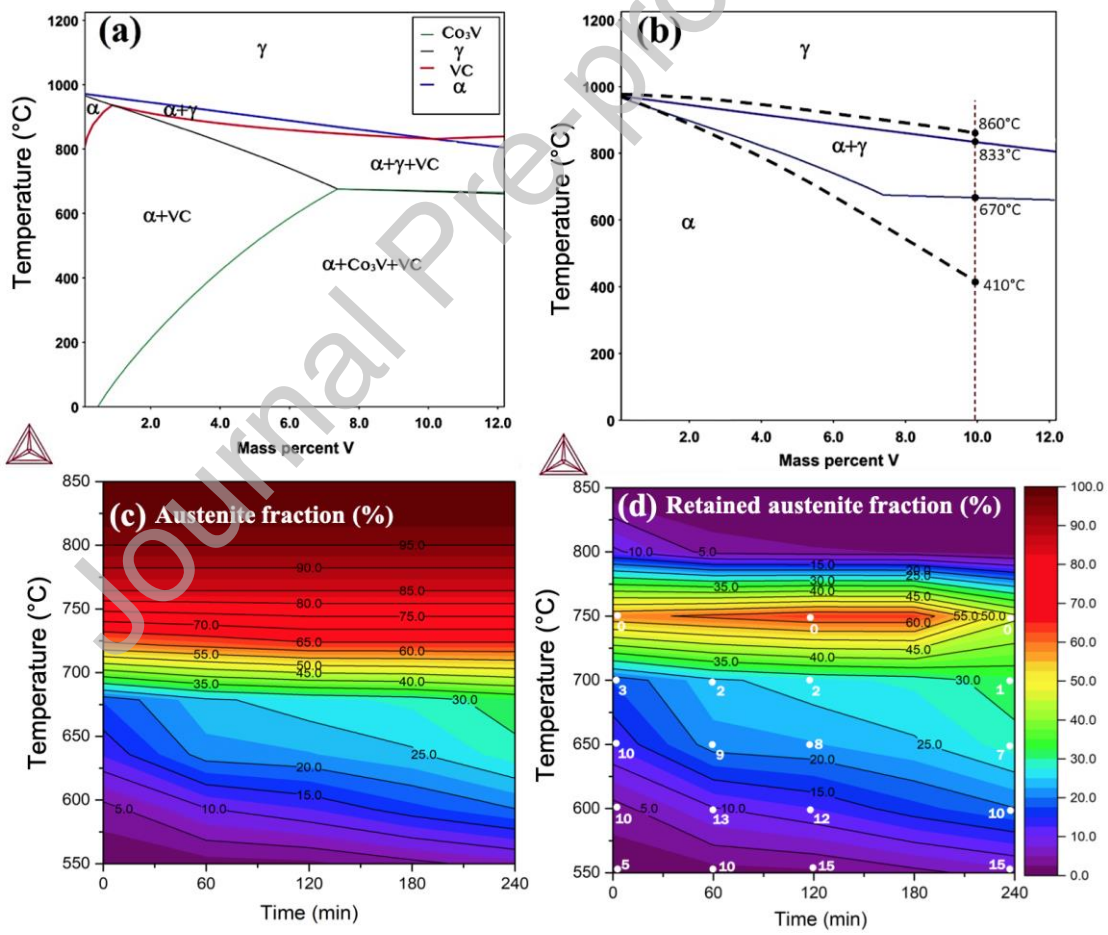

Fig. 13. Phase diagrams. (a) The equilibrium diagram for equiatomic Fe-Co-V alloy as a function of V content predicted by the ThermoCalc and (b) only two-phase α and γ regions for better clarification, ThermoCalc results and borders determined on heating superimposed from Ref. [2,10] (shown by dashed lines) are presented for comparison. Graph (c) shows the dependence of the high-

temperature fcc-austenite fraction on annealing temperature and holding time, and (d) that for the retained austenite at room temperature. Grey dots in (d) with a number indicate the presence of low-temperature hcp-austenite and its fraction (in vol.%).

In Fig. 13, two graphs (TTT-diagrams) show the influence of temperature and soaking time on the existence of high-temperature austenite. Fig. 13c exhibits the austenite phase present at a given temperature and the retained austenite at room temperature after cooling is displayed in Fig. 13d. This way, the graphs reveal the varying stability of the high-temperature austenite. In Fig. 13d, also the presence and fraction of low-temperature austenite (precipitates) are shown by dots.

Transformation of ferrite (BCC) to austenite (FCC) results in a contraction in a dilatometric sample and this is a common method to determine the start and finish temperatures of the reaction (two-phase region). If only the allotropic transformation takes place without any other concurrent phenomenon, continuous reduction in dilatation would readily be observed in dilatometric curve. However, according to Fig. 1, there is no continuous descend in the curve after the start of the contraction, and several fluctuations exist in the curve in the temperature range of 495–840 ºC. 495 ºC (Fig. 1) is the temperature where expansion slope in the dilatometric curve can be observed which might be connected with the start of the austenite formation.

Austenite grains were observed to form at grain boundaries of the ferrite phase in EBSD phase maps as well as the XRD pattern during holding at 550 ºC, but at 500 °C the amount of austenite, if any, was not enough to be visible in the XRD pattern and the austenite grains were too small to be detectable by EBSD (few percent even at 550 °C according to Table 2). We have to admit that the austenite formation in

the ordered state is a very slow process owing to a low migration rate of the boundaries [1,10], hence, a small amount of austenite would be present at around 500–550°C (Fig. 3a). Thus, it cannot be argued that the decline of the expansion in the dilatometric curve (Fig. 1) is caused by the austenite formation. We can, however, notice that in addition to the austenite transformation, nucleation and growth of $(Co,Fe)_3V$ precipitates took place simultaneously at the temperature range of 500–700 (Figs. 10a-d and 11a,b). This phenomenon is also accompanied by contraction, for the atomic packing factor of HCP is 0.74 (like FCC) while the same factor for BCC is 0.68 [44]. Also, the number of precipitates seems to be considerable (Fig. 10), so the copious precipitation of $(Co,Fe)_3V$ particles might cause such contraction.

ThermoCalc predicts the precipitates stability from room temperature up to 670 °C, with the volume fraction of 15.5% at 500°C. It is noteworthy to mention that formation of nanoscale precipitates requires short range diffusion and they form inside the deformed ferrite grains which occupy the most volume fraction of the sample. Thus, the ordered state may not affect the precipitation kinetics significantly. Nucleation of precipitates has been observed on dislocations and subgrains [3,13], so cold deformation and recovery accelerate it [3]. Contrarily, the austenite formation only takes place along grain boundaries of coarse ferrite grains and requires long rang diffusion. Therefore, in continuous heating, the role of precipitation in dilatation changes at low temperatures in the ordered state and could be more important than that of the austenite formation. SEM investigations of samples annealed at 500 °C (Fig. 11 a,b) confirmed this claim, where precipitates were only observed after 10 min annealing at 500 °C. A few grains of austenite were found in the sample annealed at 500 °C for 30 min in which the precipitates

had reasonable amount. Increasing the temperature enhances austenite formation and reduces precipitation, consequently the relative contributions will change.

Contrarily to the experimental results, which indicate low temperatures of 495–550 °C for allotropic transformation, the ThermoCalc software predicts a considerably higher start temperature of 670 °C for this reaction (Fig. 13). However, there are firm evidences from XRD and EBSD results which prove austenite formation, revealing the presence of the austenite phase at 550 ºC (Figs. 2 and 3), as well as SEM observations which ascertained austenite at 500 °C after 30 min. Thus, precipitates and austenite seem to coexist up to 670 °C.

It is worth mentioning that based on some reports, there are two temperature ranges for austenite formation in an Fe-Co-V alloy system, and accordingly, the relevant austenite has been called as low-temperature or high-temperature austenite [2,4]. Low-temperature austenite is always formed below 700 °C with the equiaxed (globular) morphology even in alloys containing 2%V. Up to now, no authors have mentioned the reason behind austenite formation at low temperatures. However, the reason for precipitation has been claimed to be decomposition of unstable martensite to ordered ferrite plus precipitates [3,4,16,17,22]. According to the current study, it can be concluded that not only precipitation, but also the formation of austenite is connected to decomposition of martensite. In other words, when unstable vanadium-rich martensite (supersaturation of vanadium in ternary Fe-Co-V system) [45], is annealed at temperatures above 500 °C, vanadium is exorcised from martensite to form a thermodynamically stable phase, i.e. ordered ferrite. Therefore, local vanadium concentration reaches high levels and reduces the temperature of

the allotropic transformation, thereby it would facilitate austenite formation. This phenomenon could take place for ternary alloys in such a way that increasing vanadium content would enhance the volume fraction of austenite. Austenite formation through this process would slow down after a while due to the transformation of vanadium-supersaturated martensite into ferrite (equilibrium phase). This can be clearly proved in two cases, in the dilatometric curve, where expansion occurred above 650 °C, and by comparing austenite fractions in the temperature range of 550–700 °C (Table 2). Afterward, the produced ferrite containing lower amount of vanadium than parent martensite, starts to transform to austenite at the lowest temperature of the two-phase region. Taking ferrite composition into account, which is around 5 at.% according to Table 3 (i.e. around 4.8 wt.%), and considering start temperature of the two-phase region in the graph presented by Sourmail [2] for this vanadium amount (dashed lines in Fig. 13b), 750 ºC would be the anticipated temperature for the lower limit of the two-phase region, and is in consistent with our results showing contraction above 750 ºC in the dilatometric curve (high temperature austenite). Moreover, coalescence of γ_2 precipitates and their dissolution in austenite, can increase the amount of austenite between 550–700 ºC (black arrows in Fig. 10).

Concerning the austenite finishing temperature, there is a contraction in section IV of the dilation plot, ending at 840 ºC (Fig. 1). According to the XRD and EBSD results the complete austenite structure is reached at temperatures between 800 and 850 ºC. Consistently, ThermoCalc predicts the temperature of 833 °C as the boundary of the $\alpha+\gamma/\gamma$ region.

Accordingly, the two-phase region of (α+γ) seems to lie on the temperature range of ~ (495–840 ºC). This region can be compared to the temperature range (410–860 ºC) presented by Sourmail [2] in his review paper (Fig. 13b). As mentioned earlier, after accomplishment of the disorder state (≥730 ºC), austenite transformation takes place faster than in the ordered state (see the fractions in Table 2). The contraction due to the onset of high-temperature austenite formation at disordered state was taken as the start temperature of austenite formation in a study of Zakharov et al. [18] for an Fe-52Co-6.85V alloy, whereas in the research performed by Hasani et al. [9] on the similar composition, the temperature range of 490–910 °C was determined as the two-phase region using dilatometric and XRD techniques. Oron et al. [14] observed the austenite phase in samples annealed at the temperature range of 600–800 ºC for an Fe-(51-52)Co-(10-11.7)V alloy. Their result is in reasonable agreement with the current study, although, they did not perform annealing treatment below 600 ºC.

4.2.2 Thermal stability of austenite

According to XRD and EBSD analyses, as the annealing temperature rises, the amount of austenite phase retained at RT increases until 750 ºC, but only a small fraction of austenite remains after annealing at 800 ºC and cooling to RT (Table 3). The structure was fully martensitic after annealing at 850°C for 120 min (Fig. 3e), i.e. the martensite finishing temperature M_f is above RT. M_f was about 100 °C according to the dilatometric curve after annealing at 1000 °C for 15 min (Fig. 1). TEM investigations, given in Figs. 7 and 8, revealed that the composition of the austenite after annealing in the two-phase region varied especially due to the

vanadium partitioning into austenite during annealing; this is also the case for cobalt but in a much lesser extent.

The stability of austenite is dependent on several factors, but mainly on chemical composition and grain size [46,47]. The other factors, morphology for instance, can be neglected, (see Refs. 46,47), for the morphology of the high-temperature austenite does not vary but remains block-like (globular). As realized, both the chemical composition of austenite and grain size vary with annealing temperature and time. We tried to get an understanding on their influence in the present alloy. M_S is a variable to characterize the thermal stability of austenite. Unfortunately, we only have one measured M_S, the value 280 °C for the austenite annealed at 1000 °C for 15 min, i.e. for a coarse-grained austenite with the ordinary alloy composition (40Fe-50Co-10V). Austenite fractions after annealing at 800 °C for various durations of 10–240 min are presented in Table 3. However, we have to notice that the temperature 800 °C lies in the two-phase region, where also the ferrite phase is present. M_S can be predicted in steels using the Koistinen-Marburger (K-M) equation [48]:

$$F_M = 1 - \exp\left[-\alpha\,(M_S - T)^{\beta}\right] \quad (1)$$

where F_M is volume fraction of martensite, T is the quenching temperature and α and β are composition-dependent fitting coefficients. According to Lee et al. [49], the parameter β has a value close to 1 and α is dependent on the chemical composition of a steel and found to be close to 0.03 for pure iron. In the case of the present alloy, no values are reported for these parameters in the literature. However, α can be determined if we take β=1 and use the experimental observation from the

dilatometric experiment (Fig. 1) which yields M_S = 280 °C and M_f = 100 °C. Assuming the austenite fraction $F_A=(1-F_M)$ at 100 °C as 1%, we would have:

$$\ln (0.01) = -\alpha (280 - 100) \quad (2)$$

Thus, α = 0.026, i.e. close to the value of 0.03. Accordingly,

$$M_S = -\ln (F_A)/0.026 + T \quad (3)$$

where T is the room temperature (24 °C) in the present experiments. Depending on the stability, this austenite has partially transformed to martensite, and the retained austenite fraction at 800 °C can be obtained from Table 2 for different annealing times (except after 4 h, when the microstructure is completely martensitic). In addition, we may assume that ferrite has no influence on the transformation of austenite to martensite in the two-phase region. Then, using Eq. (3), we can predict Ms after various holding times at 800 °C. The predicted values are listed in Table 4.

Table 4. Predicted M_S temperatures for different soaking times at 800 °C according to the K-M equation.

Annealing time at 800 °C (min)	F_A	M_S (°C)
10	0.108	110
30	0.036	152
60	0.027	163
120	0.024	167
240	0.003	247

The K-M equation presents the transformed martensite fraction from 100% austenite. However, in the present instance, ferrite also existed at 800 °C in addition to austenite, so that the martensite fractions or the retained austenite are not formed from 100% austenite rather from a smaller austenite volume. The amount of ferrite can be measured from EBSD images (light areas) like in Fig. 3d, as well as from corroded areas in SEM images of etched samples, such as in Fig. 5, it can vary locally though. Analyzing several EBSD and SEM images, the average ferrite

fraction of 15% was obtained for samples annealed at 800 °C for all holding times, whereas ThermoCalc predicts 31% of ferrite in the equilibrium state. To achieve a rough understanding on the sensitivity, we have predicted M_S assuming both the ferrite fractions of 31% and 15% (and adjusted the F_A correspondingly), and the resulted values are listed in Table 5.

Comparing the M_S values in Tables 4 and 5, it can be noticed that M_S temperatures become lower taking two-phase structure into account, but the influence is not very significant. For instance, after 120 min of soaking, the difference is only 6 °C (167 to 161 °C) and 19 °C (167 to 148 °C), as the austenite fraction decreases from 100 to 85 and 69% respectively. Nevertheless, it can be seen that M_f (M_S-180 °C) is below room temperature, so that we should have partial transformation of austenite to martensite in all instances. The observation displayed in Fig. 3d (F_A = 2.4%) is consistent with the predicted M_S of (148–161 °C), or M_f in the range of (-48–-19 °C).

Table 5. Austenite fractions at room temperature after various annealing times at 800 °C retained from austenite + ferrite structure containing 31% or 15% ferrite and predicted M_S temperatures (°C).

Annealing time at 800 °C (min)	31% ferrite assumed		15% ferrite assumed	
	F_A	M_S (°C)	F_A	M_S (°C)
10	0.177	91	0.127	103
30	0.059	133	0.042	146
60	0.044	144	0.032	157
120	0.039	148	0.028	161
240	0.005	228	0.004	241

The predicted values suggest that M_S increases with increasing annealing time, i.e. austenite stability decreases. According to Table 2, the volume fraction of austenite at 800 °C for all durations is about 85% which suggests that the chemical composition of austenite is equal. Hence, these changes in M_S value must result from the austenite grain growth as a function of holding time at 800 °C.

The K-M equation predicts the value of M_S only according the fraction of martensite (or retained austenite), but it does not account for the role of grain size. In order to demonstrate the effect of grain size on austenite stability, it is possible to predict the M_S under certain circumstances using Eq. (4) presenting an experimental relation for the M_S temperature affected by chemical composition and grain size of the austenite [47]:

$$M_S = M_{S0} - BV_\gamma^{-1/3} \quad (4)$$

Here M_{S0} depends on the alloying composition, V_γ is the volume of austenite grains in μm^3 and the coefficient B is the geometry factor [47,50].

In order to assess M_{S0}, the value of 600 °C for lath martensite was adapted from the calculations of M_S values for Fe-Co alloys from Ref. [51]. The data just covered up to 30%Co, so the value cannot be that precise. The coefficient for the powered vanadium content from the same thesis [51], is -35 °C/wt.%. Thus, excluding the potential impact of the difference of 30–50% in Co, $M_{S0} = 600 - 35\times V$ for Fe-Co-V alloys is obtained. Therefore, Eq. (4) can be written as:

$$M_S = 600 - 35\times V - 65\,(V_\gamma)^{-0.33} \quad (5)$$

Regarding 4%V in ferrite (according to Table 3) and the ferrite volume fraction of 15% in annealing at 800 °C, the vanadium content in austenite at high temperature would be around 11% and thus M_{S0} = 215 °C. Using the austenite grain sizes shown in Fig. 4b and Table 6, assuming spherical shaped grains, and B=65 μm°C, the predicted M_S values using Eq. (5) are given in Table 6. The value of B was found out by trial and error, but it can be noticed that quite a similar coefficient of B=60.5 μmK was used by Lee et al. [52] for a medium Mn steel (Ref. [49]). It can be seen that the predicted M_S is in reasonable agreement with the predicted values in Table 5, especially in the instance of short holding times (10–120 min). For experimental confirmation, we can estimate M_f , taking 180 °C as the difference between M_S and M_f according to dilatometric data, and these values are shown in Table 6. The M_S and M_f values seem quite reasonable while retained austenite fraction at 800 °C for 10, 30, 60, 120 and 240 min are 10.8, 3.6, 2.7, 2.4 and 0.3 vol.% respectively. For example, after 120 min holding, $M_S \approx 185$ °C, i.e. $M_f \approx 5$ °C, so almost complete martensitic transformation with small fraction of retained austenite could be expected during cooling to room temperature, as also experimentally observed (Fig. 3d).

From the predictions, we can realize that the real vanadium concentration in austenite has a significant impact on Ms, and, on the other hand, temperature and holding time can affect the degree of vanadium partitioning. However, much efforts would be needed to measure the data. Vanadium partitioning process yields increased vanadium contents from 10% up to as high as 25%, which means a drop in Ms by 525 °C; this can account for 35 °C drop for each weight percent of the

alloying element. On the other hand, the maximum impact that the grain size variable imposes was predicted to be only -106 °C (grain size ≈ 0.8 μm).

Table 6. Calculations for determining M_S and M_f taking austenite composition and grain size into account for various durations at 800 °C (ferrite 15%), according to Eq. (5).

Annealing time at 800 °C (min)	Austenite grain size (μm)	Vol (μm^3)	GS effect (°C)	600-35V (°C)	M_S (°C)	M_f (°C)
10	0.80	0.38	106	215	109	-71
30	1.23	0.97	66	215	149	-31
60	1.66	2.40	49	215	166	-14
120	2.70	10.3	30	215	185	5
240	3.70	26.5	22	215	193	13

Adapting Eq. (5), calculations of M_S for some other conditions were performed and the values are shown in Table 7. They forecast correctly that the structure is fully martensitic after annealing at 850 °C (grain size about 25 μm, M_S = 277 °C), while at 750 °C-120min, M_S is close to room temperature, so the martensite formation reaction just starts (no martensite seen in Fig. 3c). Accordingly, partial transformation of austenite to martensite is expected after 240 min annealing at this temperature while M_S lies on 48 °C, as it is confirmed by the formation of 18 vol.% martensite (Table 2).

Table 7. Calculations for determining M_S and M_f taking austenite composition and its grain size into account for various annealing conditions, according to Eq. (5).

Annealing condition		Vol.	V	600 – 35V	GS effect	M_S	M_f
Temp. (°C)	Time(min)	(μm^3)	(wt.%)	(°C)	(°C)	(°C)	(°C)
850	120	8181	10	250	3	247	67
800	120	10.3	11	215	30	185	5
750	120	0.34	14	110	93	17	-163
750	240	1.15	14	110	62	48	-132

4.3 Precipitation phenomenon

4.3.1 Intermetallic $(Co,Fe)_3V$ compound

According to ThermoCalc calculations, an intermetallic Co_3V -type compound, rich in Co and V, is a stable phase in ferrite at low temperatures up to 670°C (Fig. 13). Precipitation of this compound has been investigated in some studies [3,22]. Formation of these precipitates was investigated in an nearly equiatomic Fe-Co alloy containing 2%V by Ashby et al. [3]. Their results revealed that precipitation is affected by prior cold rolling. Precipitates form on dislocations as well as sub-grain boundaries and exhibit an ordered $L1_2$ structure and grow as rods in the <111> direction in the ordered ferrite. Sundar and Deevi [22] studied precipitation (termed γ_2 phase) in an Fe-41.25Co-4.46V alloy. They reported that the composition of particles formed below 700°C was $(Co,Fe)_3V$ and possessed FCC crystal structure. An improvement of ductility of the ordered structure was attributed to the fine ($\alpha'+\gamma_2$) microstructure formed during the decomposition of metastable martensite.

Anyway, despite the significant effect of these precipitates on magnetic properties of Fe-Co-V based alloys due to their paramagnetic nature [1,11–15,21,53], the precipitation phenomenon has not attracted much attention yet. Therefore, we investigated microstructural and morphological features of the precipitates as well as temperature intervals for the precipitation using various techniques. TEM investigations revealed nano-sized particles with the composition of $(Co,Fe)_3V$ and rod-shaped morphology formed inside ferrite grains coexisting with the ordered $L1_2$ globular austenite grains located along grain boundaries. According to extensive SEM study (not all images shown here), these precipitates could be observed after 10 min soaking at 550 °C. Previous studies [11–13,15,21] on ternary Fe-Co-V

system have argued that the crystal structure of these precipitates is $L1_2$ (ordered FCC) except for the work of Saito [54] on binary Co-V system, who reported that these particles are of HCP crystal structure and have the exact stoichiometric composition of the Co_3V compound. Owing to the nanometric size scale of those precipitates and overlapping the diffraction patterns of the precipitates and the surrounding matrix, we employed a deep etching technique dissolving the ferrite (actually low vanadium content phases) to patently determine the crystal structure of these precipitates. To distinguish between FCC or HCP structure, crystal rotation of about 40° was performed also for the single-phase precipitates in the etched region, which confirmed the HCP crystal structure of the present rod-shaped particles. Furthermore, the composition of the precipitates, determined in the etched region of the samples, was found to be constant $(Co,Fe)_3V$ while annealed at temperatures of 600 and 650 ºC (Table 2), whereas the composition of the austenite changed. In a number of studies [11–13,15,21], the ordered $L1_2$ austenite has been considered as precipitated particles, and this is an obvious reason for some discrepancies concerning the morphological features of these precipitates (Table 8). It is noteworthy to mention that the austenite has equiaxed morphology and at low temperatures (for example at 600 ºC in the current study) the composition of austenite is very close to that of the precipitates owing to the partitioning of V and Co elements. Thus, it appears that some authors have not distinguished the rod-shaped $(Co,Fe)_3V$ precipitates and the globular austenite phase but regarded the low-temperature austenite as precipitates with the $L1_2$ crystal structure.

At temperatures of 550 ºC and above, the hexagonal $(Co,Fe)_3V$ precipitates begin to coarsen and coalesce together and thereby convert to the $L1_2$ austenite phase

gradually. This phenomenon is demonstrated in Fig. 10 for temperatures of 550, 600, 650 and 700 ºC (annealing for 60 min) in high magnifications. It can be observed that the highest amount of rod-shaped precipitates seem to exist at the annealing temperature of 550 ºC. Also, noticing the associated peak in the XRD patterns in Fig. 2 confirms that the highest fraction of this phase existed at 550 ºC, the lowest temperature studied. ThermoCalc predicts 15.6% of Co3V at 500 °C and 13.8% at 550 °C, decreasing with increasing T. The decreasing fraction of the precipitates with increasing temperature is also seen in Fig. 10, so that just a small fraction of precipitates is left at 700 ºC, not detectable by XRD anymore. In agreement, ThermoCalc predicts 670°C as a maximum temperature for the existence of Co_3V. Thus, we can conclude that the precipitates are formed first at short holding times and then there is tendency for them to dissolve into $L1_2$ austenite. In order to confirm this claim, SEM examinations were performed for samples annealed at 500 °C for all durations and views of 10 and 240 min are presented in Fig. 11. The beginning of the formation of precipitates is evident as traces inside the ferrite. Owing to extremely fine size of the particles and therefore minimal vanadium diffusion at this stage, ferrite still has a high vanadium content so that recognizing the precipitates is cumbersome. However, a high number of images (not shown here) did not show any austenite grain formation for 10 min duration. After 30 min, some austenite grains were observed along ferrite grain boundaries growing in size and number with increasing annealing time. For better clarification, duration of 240 min with higher contrast were selected and illustrated in Fig. 11b in which both austenite grains and nano-precipitates are distinctly observable.

4.3.2 Intermetallic $(Co,Fe)V_3$ compound

We detected small precipitates rich in V forming after annealing at 850 °C and reported them as CoV_3 type compound (Fig.12). Hasani et al. [5,20] observed precipitates at and above 850 °C and connected their formation with the instability of austenite during cooling to room temperature. These particles were regarded as Co_3V type precipitates and were argued to result in depletion of V in the austenitic matrix at high temperatures. As a consequence, since V acts as austenite stabilizer, austenite would become unstable and transform to martensite upon cooling. However, the current study demonstrates that the main reason for the instability of the austenite, appearing in annealing above 750 °C, is the reduced V content due to the increasing austenite fraction with increasing annealing temperature as well as the coarsening of austenite grain size. For example, austenite became relatively instable at samples annealed at 750 °C for 240 min (around 18 vol% martensite after cooling), whereas no Co_3V or CoV_3 type precipitates were presented, but vanadium depletion and austenite grain growth took place.

Regarding the dilatometric curve, it is clear that after the contraction due to fast austenite formation above 750 ºC, there is another slope change before the completion of austenite transformation at 840 ºC. Hence, another phenomenon begins around 780 ºC and finishes at 810 ºC. To the best of authors knowledge and according to observations, there is no other phase transformations at these temperatures but the formation of CoV_3 particles (Fig. 12). Therefore, it would be reasonable to assume that this slope change designates the precipitation of those V-rich compounds. Information about this compound is very rare in the literature, but its crystal structure is BCC like that of vanadium, and it is thermodynamically stable below 1125 ºC even at room temperature [32]. After a homogenizing process at 1200 ºC for 10 hours and following

quenching to room temperature, these particles were not observed. They were not seen in microstructures after annealing at 500–750 °C either, and it seems that a temperature between 750–800 °C is required to start their formation in annealing times used in the experiments. Formation of this phase can affect the volume of a sample probably in two ways. First, formation of a BCC phase inside the FCC austenite would increase the volume. Secondly, formation of vanadium-rich particles would consume this element from the surrounding matrix and thereby increases the polymorphic transformation temperature locally at these regions. Therefore, local transformation of austenite back to ferrite would be possible adjacent to precipitates which also leads to a volume increase in a dilatometric sample. With further heating, the locally formed ferrite will transform to austenite (above 810 ºC) along with remained ferrite, causing contraction in the dilatation, but those particles remain stable until 1125 ºC. This is a plain hypothesis which needs more studies to be confirmed.

Finally, it should be mentioned that ThermoCalc predicted formation of vanadium carbide (VC) owing to the existence of very low amount of carbon in the alloy composition. Thermodynamically stable state for this compound in the studied alloy was predicted to be below 833 ºC. However, no carbide was observed probably due to high purity of the materials and the very low carbon content (Table 1).

4.4 Comparison between present results and previous data

In spite of numerous studies, there were still unclear issues in the annealing behavior of Fe-Co-V alloys. As mentioned, several concurrent phenomena occurring during annealing process makes it difficult to determine facts for each single transformation. To represent the main deficits and inconsistencies, previous data on those phenomena in

ternary Fe-Co-V alloy systems were collected from the literature and listed in Table 8. In the present study, the existence of most disagreements in these previous works could be explained.

As an example, Chen [19], Duckham et al. [42] and Zakharov [18] could not observe the precipitation phenomenon in their alloys. Many researchers have reported it, but even these reports seem to be inconsistent concerning some features. For instance, the temperature intervals of the precipitation vary as well as the morphology and crystal structure of the precipitate. Some authors have determined the crystal structure as simple FCC, while some others considered it as ordered $L1_2$. Meanwhile, the morphology of these precipitates has been reported to be fibrous or/and equiaxed.

The precipitation reaction seems to take place in all Fe-Co-V ternary systems in the approximate temperature range of 500–700 °C. Particles form inside initial ferrite grains with nanometric size and rod-shaped morphology. The fine size might be a reason that some authors did not detect them. The EBSD method as well as metallography are not capable to resolve those precipitates due to limited resolution. Moreover, X-ray diffraction cannot reflect the related peak in low-vanadium alloys due to a small fraction of precipitates.

According to some inconsistent reports on morphological features, it seems that some authors could not distinguish between low-temperature austenite with the equiaxed morphology and rod-shaped precipitates and this is the reason for discrepancies concerning the morphology of the forming species. Although the crystal structure of precipitates is HCP, yet in certain directions the diffraction

patterns of HCP and FCC are identical. Moreover, owing to the very small size of precipitates as well as their small fraction in low-vanadium alloys, they cannot be distinguished by X-ray diffraction. Some authors have reported the $L1_2$ crystal structure for the precipitates because erroneously considered the low-temperature austenite as precipitates. Pitt and Rawlings [11] determined two temperature ranges in which rod-shaped and equiaxed precipitates have formed. However, it seems that the equiaxed grains were not precipitates but austenite.

In addition to contradictory reports about the precipitation reaction, there are also inconsistent conclusions concerning the temperature intervals of the ferrite to austenite transformation. For example, Zakharov et al [18] determined the temperature intervals of austenite transformation in the range of 800–912 °C for Fe-52Co-7V alloy while the range of 490–910 °C was specified by Hasani et al [9] for a similar composition.

As already pointed out, there are two temperature ranges for the austenite formation in an Fe-Co-V alloy system, and consistently the austenite has been called as low-temperature or high-temperature austenite [2,4]. Low-temperature austenite is always formed below 700 °C with an equiaxed (globular) morphology and $L1_2$ crystal structure, even for alloys containing 2%V, owing to decomposition of supersaturated martensite as well as converting precipitates to austenite, as explained in sections 4-2-1 and 3-5 respectively. The low-temperature austenite has a composition very close to $(Co,Fe)_3V$ in the early stages of formation (at the temperature range of 500–550 °C). However, the composition of the low-temperature austenite is not constant but changes with increasing the annealing

temperature. In alloys containing a low amount of vanadium, not only the fraction of low-temperature austenite is negligible, but also it is of fine grain type, so that some authors could not recognize it through XRD, metallography or magnetic measurements.

On the other hand, the high-temperature austenite possesses disordered FCC lattice structure and the temperature interval may vary between alloys depending on the vanadium content of the alloy: (876–932 °C) for Fe-49Co-2V [19], (789–910 °C) for Fe-49.6Co-7.15V [9] and (750–840 °C) for the present alloy.

We also discovered the precipitation of particles rich in V and depleted of Fe and Co in austenite at high temperatures. Unknown precipitates were reported by Kawahara [55] after annealing a cold-rolled Fe-Co-2V alloy at 900 °C for 1 hour, which can be connected with the precipitates detected in the current study. Although most of the researches have reported temperatures below 700 °C for the temperature range of $(Fe,Co)_3V$ precipitation, Hasani et al. [20] devoted the temperature above 850 °C to that. However, in the present study, the precipitates formed above 800 °C were supposed to be of CoV_3 type. Thus, it seems that Hasani et al. [20,22] erroneously considered CoV_3 precipitates as Co_3V compound.

Table 8. Temperature intervals of various processes (in °C) and crystal structure and morphological features of precipitates in Fe-Co-V based alloys.

Alloy composition	Ordering trans. (temperature range on heating)	Allotropic trans. (temperature range on heating)	Recrystallization (start and finish temperature)	Precipitation (temperature range, structure, morphology)	Reference
Fe-48.68Co-1.89V-0.3Nb	438–650	—	438–650	No precipitation	Duckham et al. [42]
Fe-49Co-2V	~700	895–955	—	No precipitation	Chen [19]

Fe-50.33Co-2V	—	(850-875) – (900-950)	—	(477–627), $L1_2$, rod-shaped	Ashby et al. [3]
Fe-49Co-2V	—	—	650–750	(500–600), $L1_2$, —	Couto & Ferreira [56]
Fe-49Co-2V	—	870–950	—	(500–700), FCC, rod-shaped	Kuroda & Ogawa [57]
Fe-49Co-2V	—	—	680–750	(550–750), $L1_2$, < 680 ºC rod-shaped, > 680 ºC equiaxed	Pitt & Rawlings [11]
Fe-49Co-2V	—	—	670–710	—	Thornburg [58]
Fe-49Co-2.2V		—	700 (completed)	< 700, FCC, globular (0.1-0.4µm)	Fiedler & Davis [12]
Fe-48.3Co-2.5V	—	900-950	—	(600–700), FCC, —	Bennett & Pinnel [4]
Fe-48.88Co-2.8V	—	600–900	700 (completed)	(600–700), FCC, —	Pinnel et al. [34]
Fe-42.27Co-4.33V-0.7Si-0.48Mn	—	—	—	(580 ºC, fibrous – 610 ºC, equiaxed), —	Wu et al. [13]
Fe-41.25Co-4.45V	675	940–960	—	< 700, FCC, —	Sundar & Deevi [22]
Fe-52Co-6.85V	550–700	800–912	—	No precipitation	Zakharov et al. [18]
Fe-49.6Co-7.15V	330–734	490–910	500–870	≥ 850, $L1_2$, grainy	Hasani et al. [9,20,38]
Fe-(51-52)Co-(10-11.7)V	600–700	600–800	> 600 ºC(2h)	(600–660), FCC, globular	Oron et al. [14]
Fe-49.8Co-9.96V	320–(700-750)	(500-550) – (800-850)	> 600 (1h) – never completed	—	Kamali et al. [10]
Fe-49.8Co-9.96V	350 - 750	500 – 840	—	495 – 700, HCP, rod-shaped, >800°C, BCC, roundish	Present study

5 Summary and conclusions

The experimental study of the phenomena taking place during annealing an Fe-50Co-10V alloy has been carried out in order to clarify the temperature ranges of transformations as well as crystal structure and morphological features of different phases and precipitated particles. In this regard, in addition to a dilatometric run, numerous heat treatment experiments were conducted on 86% cold-rolled sheets in

a temperature range of 500–850 °C and durations of 10–240 min. Owing to the simultaneous occurrence of ordering, precipitation and polymorphic phase transformation, various techniques incorporating dilatometry, XRD, TEM, EBSD, SEM and ThermoCalc predictions were employed to enable investigation on each phenomenon separately. Based on the measurements, the following main results can be listed:

1. The ordering transition during continuous heating of cold-rolled disordered BCC martensitic structure becomes visible at 350 ºC in a dilatometric curve, and based on XRD patterns, ordering reaches the highest degree at 600 ºC, weakening with further heating, and finally the order disappears at a temperature close to 750 ºC.

2. Based on the dilatometric curve, precipitation of nano-sized, rod-shaped particles with the composition of $(Co,Fe)_3V$ starts at 495 ºC, occurring inside the deformed initial ferrite (martensite) grains, as seen by SEM at 500 °C. The crystal structure of particles is HCP as determined by TEM. The highest volume fraction of precipitates is obtained at 550 °C, the lowest temperature studied, and these precipitates dissolve gradually into austenite through increasing annealing temperatures so that no precipitates exist above 700 ºC.

3. According to EBSD, TEM and SEM examinations, concurrently with the precipitation, the formation of austenite starts at 500°C with equiaxed grain morphology and ordered $L1_2$ crystal structure, by nucleation mostly along boundaries of initial ferrite grains. Two temperature ranges were found with respect to the existence of the austenite, called low- and high-temperature austenite. The

former nucleates and grows due to decomposition of martensite and the later starts at the lowest temperature of the two-phase region of remained ferrite, containing a lower amount of vanadium than martensite, and austenite. The volume fraction of austenite as well as its grain size increase significantly in the disordered state so that the completion of the phase transformation occurs at 840 ºC. Austenite forms as an ordered phase at low temperatures and a disordered structure at 750 °C and above. Due to partitioning of V and Co into austenite during annealing, determined by TEM elemental mapping, austenite can be stable and remain down to room temperature. At 750 °C and above, depending on annealing duration, the thermal stability of austenite is decreased due to lower V enrichment and coarsened grain size, which results in transformation of some austenite to martensite upon cooling.

4. The formation of micron-sized precipitates with BCC crystal structure rich in V and depleted of Fe and Co, supposed to be $(Co,Fe)V_3$ compound, were observed in austenite at 850 °C. The fifth deviation in the dilatometric curve, starting as an expansion from 778 ºC, was attributed to the precipitation of these particles with the BCC crystal structure inside austenite grains as well as local transformation of austenite to ferrite due to depletion of vanadium around those vanadium rich particles.

5. The present work has employed various research techniques, clarified especially the precipitation of $(Co,Fe)_3V$ and formation of austenite in deformed ordered ferrite at temperatures below 750 °C. It also analyses the stability of austenite, based on V enrichment and grain size. Furthermore, it reveals that the order to disorder transition for austenite takes place in the same temperature range as for ferrite (between 700 and

750 °C), related to emergence of superlattice reflection at 41.5° in XRD patterns. Also, the reflections at 48.6º and 56.5º propose the existence of $(Co,Fe)_3V$ precipitates.

Acknowledgments

MRK is grateful for financial support from the Iranian government for his research stay at the University of Oulu and for facilities and equipment provided by the University of Oulu for performing this study. LPK and JK acknowledge the support of the Academy of Finland for the "Genome of Steel" project #311934

Authors contributions

Mohammad R. Kamali performed all experiments, analyzed the data, prepared figures and wrote the main part of the draft manuscript. Ali R. Mashreghi designed the experiments, supervised the project and commented the results. Pentti Karjalainen supervised the study, contributed to discussions by commenting, drawing conclusions and checking and revising the manuscript. Saeed Hasani supervised the project, designed the experiments and commented the results. Sami Saukko performed TEM imaging and diffraction patterns and contributed to analyses of them. Vahid Javaheri participated preparation of figures and ThermoCalc calculations. Jukka Komi contributed to discussions by commenting and general supervising.

Declaration of Competing Interest

The authors declare that they have no known competing financial interests or personal relationships that could have appeared to influence the work reported in this paper.

Data availability

The raw/processed data required to reproduce these findings cannot be shared at this time due to technical or time limitations.

References

[1] R.S. Sundar, S.C. Deevi, Soft magnetic FeCo alloys: Alloy development, processing, and properties, Int. Mater. Rev. 50 (2005) 157–192. doi:10.1179/174328005X14339.

[2] T. Sourmail, Near equiatomic FeCo alloys: Constitution, mechanical and magnetic properties, Prog. Mater. Sci. 50 (2005) 816–880.

doi:10.1016/j.pmatsci.2005.04.001.
[3] J.A. Ashby, H.M. Flower, R.D. Rawlings, Gamma phase in an Fe-Co-2%V alloy, Met. Sci. 11 (1977) 91–96. doi:10.1179/msc.1977.11.3.91.
[4] J.E. Bennett, M.R. Pinnel, Aspects of phase equilibria in Fe/Co/2.5 to 3.0% V alloys, J. Mater. Sci. 9 (1974) 1083–1090. doi:10.1007/BF00552822.
[5] S. Hasani, M. Shamanian, A. Shafyei, P. Behjati, J.A. Szpunar, M. Fathi-moghaddam, Nano / sub-micron crystallization of Fe-Co-7.15V alloy by thermo-mechanical process to improve magnetic properties, Mater. Sci. Eng. B. 190 (2014) 96–103. doi:10.1016/j.mseb.2014.09.013.
[6] M. Matsuda, K. Yamashita, R. Sago, K. Akamine, K. Takashima, M. Nishida, Development of ductile B2-Type Fe-Co based alloys, Mater. Trans. 53 (2012) 1826–1828. doi:10.2320/matertrans.M2012205.
[7] K. Kawahara, Effect of additive elements on cold workability in FeCo alloys, J. Mater. Sci. 18 (1983) 1709–1718. doi:10.1007/BF00542066.
[8] S. Hasani, A. Shafyei, M. Shamanian, P. Behjati, H. Mostaan, T. Juuti, J.A. Szpunar, Correlation between magnetic properties and allotropic phase transition of Fe–Co–V alloy, Acta Metall. Sin. (English Lett). 28 (2015) 1055–1058. doi:10.1007/s40195-015-0294-9.
[9] S. Hasani, M. Shamanian, A. Shafyei, P. Behjati, J.A. Szpunar, Non-isothermal kinetic analysis on the phase transformations of Fe-Co-V alloy, Thermochim. Acta. 596 (2014) 89–97. doi:10.1016/j.tca.2014.09.020.
[10] M.R. Kamali, L.P. Karjalainen, A.R. Mashregi, S. Hasani, V. Javaheri, J. Kömi, Reobservations of ferrite recrystallization in a cold-rolled ordered Fe-50Co-10V alloy using the EBSD method, Mater. Charact. 158 (2019) 109962. doi:10.1016/j.matchar.2019.109962.
[11] C.D. Pitt, R.D. Rawlings, Microstructure of Fe-Co-2V and Fe-Co-V-Ni alloys containing 1·8–7·4 wt-%Ni, Met. Sci. 15 (1981) 369–376. doi:10.1179/030634581790426912.
[12] H.C. Fiedler, A.M. Davis, The formation of gamma phase in vanadium permendur, Metall. Trans. 1 (1970) 1036–1037. doi:10.1007/BF02811792.
[13] L. Wu, J. Chen, Z. Du, J. Wang, Microstructures of ultra-fine grained FeCoV alloys processed by ECAP plus cold rolling and their evolutions during tempering, Trans. Nonferrous Met. Soc. China. 20 (2010) 602–606. doi:10.1016/S1003-6326(09)60185-0.
[14] M. Oron, S. Shtrikman, D. Treves, Study of Co-Fe-V permanent magnet alloys (Vicalloys), J. Mater. Sci. 4 (1969) 581–591. doi:10.1007/BF00550114.
[15] V.I. Zel'dovich, Y.S. Samoylova, V.D. Sadovskiy, Morphological features of the formation of a gamma phase in deformed iron-cobalt-vanadium alloys, Phys. Met. Met. 42 (1976) 90–96.
[16] S. Mahajan, M. Pinnel, J. Bennet, Influence of heat treatments on microstructures in an Fe-Co-V alloy, Metall. Trans. 5 (1974) 1263–1272. doi:10.1007/BF02646609.
[17] M.R. Pinnel, J.E. Bennett, Correlation of magnetic and mechanical properties with microstructure in Fe/Co/2-3 pct V alloys, Metall. Trans. 5 (1974) 1273–1283. doi:10.1007/BF02646610.
[18] V.M. Zakharov, M.A. Libman, E.I. Estrin, On the role of atomic ordering in the formation of a high-coercivity state in iron-cobalt-vanadium alloys, Phys. Met. Metallogr. 113 (2012) 43–47. doi:10.1134/s0031918x12010152.
[19] C.W. Chen, Metallurgy and magnetic properties of an Fe-Co-V alloy, J. Appl. Phys. 32 (1961) S348–S355. doi:10.1063/1.2000465.

[20] S. Hasani, M. Shamanian, A. Shafyei, P. Behjati, M. Nezakat, M. Fathi-Moghaddam, J.A. Szpunar, Influence of annealing treatment on micro/macro-texture and texture dependent magnetic properties in cold rolled FeCo–7.15V alloy, J. Magn. Magn. Mater. 378 (2015) 253–260. doi:10.1016/j.jmmm.2014.11.050.

[21] V.I. Zel'dovich, V.M. Schastilivtsev, Y.S. Samoylova, V.D. Sadovskiy, Morphology of gamma phase formation in Vicalloy 1, Phys. Met. Metallogr. 40(1) (1975) 122–130.

[22] R.S. Sundar, S.C. Deevi, Effect of heat-treatment on the room temperature ductility of an ordered intermetallic Fe-Co-V alloy, Mater. Sci. Eng. A. 369 (2004) 164–169. doi:10.1016/j.msea.2003.11.004.

[23] J.O. Andersson, T. Helander, L. Höglund, P. Shi, B. Sundman, Thermo-Calc & DICTRA, computational tools for materials science, Calphad Comput. Coupling Phase Diagrams Thermochem. 26 (2002) 273–312. doi:10.1016/S0364-5916(02)00037-8.

[24] G.B. Chon, K. Shinoda, S. Suzuki, B. Jeyadevan, Order-disorder transformation in Fe50Co50 particles synthesized by polyol process, Mater. Trans. 51 (2010) 707–711. doi:10.2320/matertrans.M2009251.

[25] Y.I. Ustinovshchikov, Ordering–separation phase transitions in a Co3V alloy, Russ. Metall. 2017 (2017) 24–30. doi:10.1134/S0036029517010116.

[26] J. Wu, P.J. Wray, C.I. Garcia, M. Hua, A.J. Deardo, Image quality analysis: a new method of characterizing microstructures, ISIJ Int. 45 (2005) 254–262. doi:10.2355/isijinternational.45.254.

[27] L. Ryde, Application of EBSD to analysis of microstructures in commercial steels, Mater. Sci. Technol. 22 (2006) 1297–1306. doi:10.1179/174328406X130948.

[28] C. Zhao, C. Zhang, W. Cao, Z. Yang, H. Dong, Y. Weng, Austenite thermal stabilization through the concentration of manganese and carbon in the 0.2C-5Mn steel, ISIJ Int. 54 (2014) 2875–2880. doi:10.2355/isijinternational.54.2875.

[29] X. Zhao, Y. Zhang, C. Shao, W. Hui, H. Dong, Thermal stability of retained austenite and mechanical properties of medium-Mn steel during tempering treatment, J. Iron Steel Res. Int. 24 (2017) 830–837. doi:10.1016/S1006-706X(17)30123-1.

[30] H.S. Yang, H.K.D.H. Bhadeshia, Austenite grain size and the martensite-start temperature, Scr. Mater. 60 (2009) 493–495. doi:10.1016/j.scriptamat.2008.11.043.

[31] P.J. Brofman, G.S. Ansell, On the effect of fine grain size on the Ms temperature in Fe-27Ni-0.025C alloys, Metall. Trans. A. 14 (1983) 1929–1931. doi:10.1007/BF02645565.

[32] G.V. Raynor, V.G. Rivlin, Critical evaluation of constitution of cobalt-iran-vanadium system, Int. Met. Rev. 28 (1983) 211–227. doi:10.1179/imtr.1983.28.1.211.

[33] C. Wang, C. Zhao, Y. Lu, T. Li, D. Peng, J. Shi, X. Liu, Experimental observation of magnetically induced phase separation and thermodynamic assessment in the Co–V binary system, Mater. Chem. Phys. 162 (2015) 555–560. doi:10.1016/j.matchemphys.2015.06.028.

[34] M. Pinnel, S. Mahajan, J. Bennett, Influence of thermal treatments on the mechanical properties of an Fe-Co-V alloy (remendur), Acta Metall. 24 (1976) 1095–1106. doi:10.1016/0001-6160(76)90026-2.

[35] D.W. Clegg, R.A. Buckley, The disorder → order transformation in Iron–cobalt

based alloys, Met. Sci. J. 7 (1973) 48–54. doi:10.1179/030634573790445541.
[36] F.J. Humphreys, M. Hatherly, Recrystallization of ordered materials, in: Recryst. Relat. Annealing Phenom., 2004: pp. 269–283.
[37] M. Rajkovic, R.A. Buckley, Ordering transformations in Fe-50Co based alloys, Met. Sci. 15 (1981) 21–29. doi:10.1179/msc.1981.15.1.21.
[38] S. Hasani, M. Shamanian, A. Shafyei, P. Behjati, H. Mostaan, P. Sahu, J.A. Szpunar, Electron microscopy study on grain boundary characterizations of Fe–Co–V alloy during annealing, Vacuum. 114 (2015) 1–5. doi:10.1016/j.vacuum.2014.12.025.
[39] R.A. Buckley, Ordering and recrystallization in Fe-50Co-0.4%Cr, Met. Sci. 13 (1979) 67–72. doi:10.1179/msc.1979.13.2.67.
[40] P. Moine, J.P. Eymery, P. Grosbras, The effects of short-range order and long-range order on the equilibrium configuration of superdislocations in Fe-Co : 2 at% V - Consequences on flow stress, Phys. Status Solidi. 46 (1971) 177–185. doi:10.1002/pssb.2220460115.
[41] N. Stoloff, R. Davies, The plastic deformation of ordered FeCo and Fe3 Al alloys, Acta Metall. 12 (1964) 473–485. doi:10.1016/0001-6160(64)90019-7.
[42] A. Duckham, D. Zhang, D. Liang, V. Luzin, R. Cammarata, R.. Leheny, C. Chien, T. Weihs, Temperature dependent mechanical properties of ultra-fine grained FeCo–2V, Acta Mater. 51 (2003) 4083–4093. doi:10.1016/S1359-6454(03)00228-3.
[43] J.F. Dinhut, J.P. Eymery, P. Moine, Plastic deformation and brittleness of Fe-Co-V, Phys. Status Solidi. 12 (1972) 153–161. doi:10.1002/pssa.2210120115.
[44] J. William, D. Callister, D.G. Rethwisch, Material science and engineering, An introduction, Wiley; 9 edition, 2010.
[45] C.M. Orrock, The microstructure and properties of equiatomic iron-cobalt magnetic alloys with alloying additions, University of London, 1985.
[46] E. Jimenez-Melero, N.H. van Dijk, L. Zhao, J. Sietsma, S.E. Offerman, J.P. Wright, S. van der Zwaag, Martensitic transformation of individual grains in low-alloyed TRIP steels, Scr. Mater. 56 (2007) 421–424. doi:10.1016/j.scriptamat.2006.10.041.
[47] E. Jimenez-Melero, N.H. van Dijk, L. Zhao, J. Sietsma, S.E. Offerman, J.P. Wright, S. van der Zwaag, Characterization of individual retained austenite grains and their stability in low-alloyed TRIP steels, Acta Mater. 55 (2007) 6713–6723. doi:10.1016/j.actamat.2007.08.040.
[48] D.P. Koistinen, R.E. Marburger, A general equation prescribing the extent of the austenite-martensite transformation in pure iron-carbon alloys and plain carbon steels, Acta Metall. 7 (1959) 59–60. doi:10.1016/0001-6160(59)90170-1.
[49] S. Lee, S. Shin, M. Kwon, K. Lee, B.C. De Cooman, Tensile properties of medium Mn steel with a bimodal UFG $\alpha + \gamma$ and coarse δ-ferrite microstructure, Metall. Mater. Trans. A. 48 (2017) 1678–1700. doi:10.1007/s11661-017-3979-z.
[50] J.R.C. Guimaraes, J.C. Gomes, A metallographic study of the influence of the austenite grain size on martensite kinetics, Acta Met. 26 (1978) 1591–1596.
[51] A. Hanumantharaju, Thermodynamic modelling of martensite start temperature in commercial steels, Doctoral thesis, KTH Royal Institute of Technology, Stockholm, Sweden, 2017. https://pdfs.semanticscholar.org/45f5/2ecd812ca99658c7c7d32236155e5ed8a15c.pdf.
[52] S. Lee, S.J. Lee, S. Santhosh Kumar, K. Lee, B.C.D. Cooman, Localized deformation in multiphase, ultra-fine-grained 6 Pct Mn transformation-induced

plasticity steel, Metall. Mater. Trans. A 42 (2011) 3638–3651. doi:10.1007/s11661-011-0636-9.

[53] G. Gorodetsky, S. Shtrikman, F.P.R.E. Sse, D.C.A. Tho, Studies of magnetic hardness in Vicalloy using the Mössbauer effect, 3981 (1967). doi:10.1063/1.1709050.

[54] S. Saito, The crystal structure of VCo3, Acta Crystallogr. 12 (1959) 500–502. doi:10.1107/S0365110X59001517.

[55] K. Kawahara, Structures and mechanical properties of an FeCo-2V alloy, J. Mater. Sci. 18 (1983) 3427–3436. doi:10.1007/BF00544171.

[56] A.A. Couto, P.I. Ferreira, Phase transformations and properties of Fe - Co alloys, J. Mater. Eng. 11 (1989) 31–36. doi:10.1007/BF02833751.

[57] C. Kuroda, T. Ogawa, Electron microscope observation of γ phase precipitation in vanadium permendur, Jpn. J. Appl. Phys. 5 (1966) 733–734. doi:10.1143/JJAP.5.733.

[58] D.R. Thornburg, High-strength high-ductility cobalt-iron alloys, J. Appl. Phys. 40 (1969) 1579–1580. doi:10.1063/1.1657779.

Graphical abstract

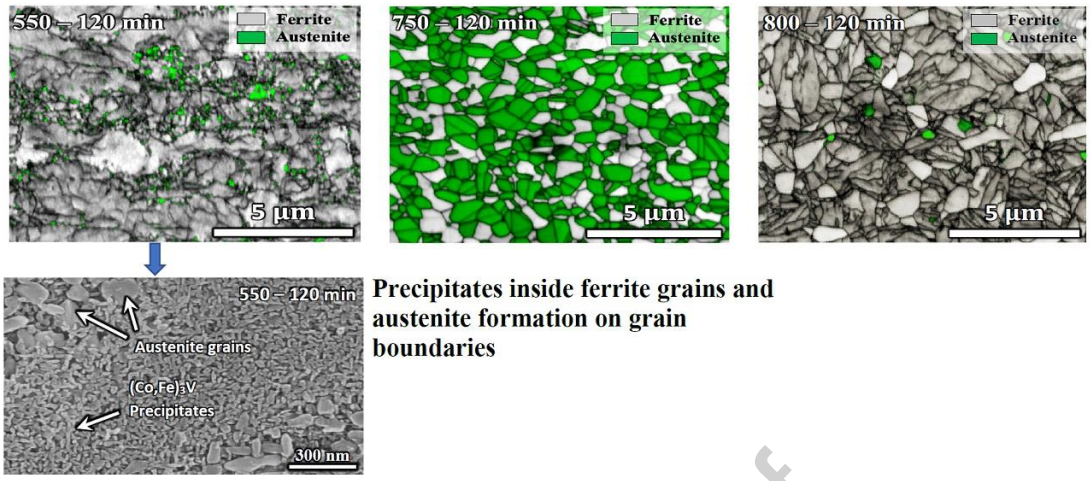

Precipitates inside ferrite grains and austenite formation on grain boundaries